AD

TECHNICAL REPORT ARCCB-TR-03013

DESIGN, TESTING, AND SIMULATION OF AN EXPERIMENTAL 105-MM M35 FIRE OUT-OF-BATTERY (FOOB) DIRECT FIRE GUN

RONALD GAST
ERIC KATHE
MICHAEL GULLY
ROBERT DUROCHER
KENNETH OLSEN
STEVEN PIGLIAVENTO

SEPTEMBER 2003

US ARMY ARMAMENT RESEARCH,
DEVELOPMENT AND ENGINEERING CENTER
Close Combat Armaments Center
Benét Laboratories
Watervliet, NY 12189-4000

TACOM-ARDEC

BENÉT Labs

APPROVED FOR PUBLIC RELEASE; DISTRIBUTION UNLIMITED

DISCLAIMER

The findings in this report are not to be construed as an official Department of the Army position unless so designated by other authorized documents.

The use of trade name(s) and/or manufacturer(s) does not constitute an official endorsement or approval.

DESTRUCTION NOTICE

For classified documents, follow the procedures in DoD 5200.22-M, Industrial Security Manual, Section II-19, or DoD 5200.1-R, Information Security Program Regulation, Chapter IX.

For unclassified, limited documents, destroy by any method that will prevent disclosure of contents or reconstruction of the document.

For unclassified, unlimited documents, destroy when the report is no longer needed. Do not return it to the originator.

REPORT DOCUMENTATION PAGE

Form Approved
OMB No. 0704-0188

1. AGENCY USE ONLY *(Leave Blank)*	2. REPORT DATE	3. REPORT TYPE AND DATES COVERED
	September 2003	Final

4. TITLE AND SUBTITLE
DESIGN, TESTING, AND SIMULATION OF AN EXPERIMENTAL 105-MM M35 FIRE OUT-OF-BATTERY (FOOB) DIRECT FIRE GUN

5. FUNDING NUMBERS
AMCMS No. 21 3 2040 36D 6D03
P6330042321

6. AUTHORS
Ronald Gast, Eric Kathe, Michael Gully,
Robert Durocher, Kenneth Olsen, Steven Pigliavento

7. PERFORMING ORGANIZATION NAME(S) AND ADDRESS(ES)
U.S. Army ARDEC
Benet Laboratories, AMSTA-AR-CCB-O
Watervliet, NY 12189-4000

8. PERFORMING ORGANIZATION REPORT NUMBER
ARCCB-TR-03013

9. SPONSORING / MONITORING AGENCY NAME(S) AND ADDRESS(ES)
U.S. Army ARDEC
Close Combat Armaments Center
Picatinny Arsenal, NJ 07806-5000

10. SPONSORING / MONITORING AGENCY REPORT NUMBER

11. SUPPLEMENTARY NOTES

12a. DISTRIBUTION / AVAILABILITY STATEMENT
Approved for public release; distribution unlimited.

12b. DISTRIBUTION CODE

13. ABSTRACT *(Maximum 200 words)*

The work reported herein details the operation, simulation, testing, and shortcomings of a direct fire weapon (105-mm M35) that has been modified to operate in a fire out-of-battery (FOOB) mode. In FOOB mode, the firing sequence is radically different than that for a conventional weapon. The gun is captured and preloaded in its out-of-battery position prior to firing. This position compares to a conventional system's maximum recoil location. When unlatched, forward momentum is imparted to the recoiling parts, which will eventually be opposed by the ballistic force imparted by firing a round. The ballistic impulse imparted to the gun reverses the momentum and returns the recoiling parts to their latched position ready for the next round. Although the total momentum imparted to the system is not changed, the FOOB approach could theoretically reduce the transmitted loads to the mount structure by 75 percent.

14. SUBJECT TERMS
Fire Out-of-Battery, Soft-Recoil, Recoil Simulation, Tank Weapon,
105-mm M35 Gun, Recoil Test, Ballistic Impulse, Dynamic Simulation

15. NUMBER OF PAGES
52

16. PRICE CODE

17. SECURITY CLASSIFICATION OF REPORT	18. SECURITY CLASSIFICATION OF THIS PAGE	19. SECURITY CLASSIFICATION OF ABSTRACT	20. LIMITATION OF ABSTRACT
UNCLASSIFIED	UNCLASSIFIED	UNCLASSIFIED	UL

TABLE OF CONTENTS

LIST OF ILLUSTRATIONS

BACKGROUND

Description of Conventional Recoil Versus Fire Out-Of-Battery (FOOB)

The function of a conventional recoil system is to reshape the highly impulsive ballistic pulse into one containing a much lower force level spread over a longer time duration. In addition, it must store enough energy such that the recoiling parts may be returned to their in-battery position ready for the next firing. Both recoil and counterrecoil deceleration must be relatively constant such that high magnitude inertia forces are not imparted to the stationary parts during any phase of the operation. The upper portion of Figure 1 contains a schematic of a weapon highlighting the three major components; namely, recoiling parts, stationary parts, and recoil system. The recoil system may be further separated into a recoil brake and recuperator. Relative force trajectories that drive the gun and resist its motion are shown below the components.

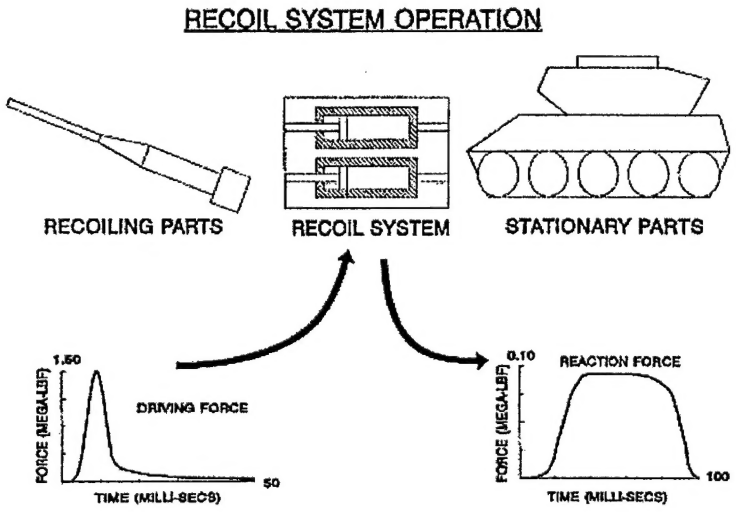

Figure 1. Schematic of a conventional recoil system.

The function of the recoil brake is to provide the bulk of the retarding forces. This is accomplished by metering flow through a travel-dependent orifice. The metering process causes the development of a back pressure, which opposes the forces on and momentum of the recoiling mass. The orifice is designed such that the force response is rather constant over time and operating stroke. The energy absorbed during this process is converted into heat, manifested by a temperature rise in the brake fluid, then conducted to the structure, and eventually dissipated to the environment. The recuperator unit is nothing more than a mechanical or gas spring. Its function is to extract and retain enough of the recoil energy during compression such that upon decompression, the recoiling parts are driven back to their in-battery position. The force level for this component is much less than that of the brake unit, moreover, little or no energy is lost during this process.

A first-order relatively conservative relationship among the ballistic pulse, recoiling weight, and recoil travel is contained in a simple equation as

$$F_r = \frac{I_b^2}{2mL} \tag{1}$$

where

F_r = maximum recoil force (lbf)
I_b = impulse from the ballistic pressure (lbf-sec)
m = mass of recoiling parts (slug)
L = length of recoil stroke (inch)

When one uses this equation, the computed maximum recoil force may be as much as 20 percent higher than that for an actual recoil system.

The impulse in this case is the integral of the ballistic force over time, including pressure blowdown subsequent to projectile exit. The force is directly proportional to the square of the impulse and inversely proportional to both the mass and recoil length. A recoil system cannot reduce the ballistic impulse imparted to the system, but may alter the force distribution, which is eventually felt by the nonrecoiling parts (i.e., turret and vehicle). To use this equation, one must assume that the gun is stationary when the ballistic charge is ignited. That is, the recoiling mass begins from rest. The force developed (F_r) will act over the full length of recoil and arrest the recoiling parts at the distance (L). If unrestrained, the maximum recoil velocity would be the ratio of the impulse to the recoiling mass (impulse = mass x velocity). The challenge is to design a braking system that can robustly reproduce the rather constant force distribution shown in Figure 1.

In a FOOB application, the firing sequence is radically different, as shown in Figure 2. The gun is latched and preloaded in its out-of-battery position prior to firing. This position compares to the conventional system's maximum recoil location. When unlatched, forward momentum is imparted to the recoiling parts (via an actuator such as a gas recuperator or mechanical spring). When the gun's forward velocity is equal to one-half of the maximum velocity it would have achieved under conventional operation, the gun is fired. The ballistic impulse imparted to the gun reverses the momentum and returns the recoiling parts to their latched position ready for the next round. For a given recoil mass and travel, the FOOB approach could theoretically reduce the transmitted loads by 75 percent. (For an in-depth coverage of a FOOB gun system, consult Reference 1.)

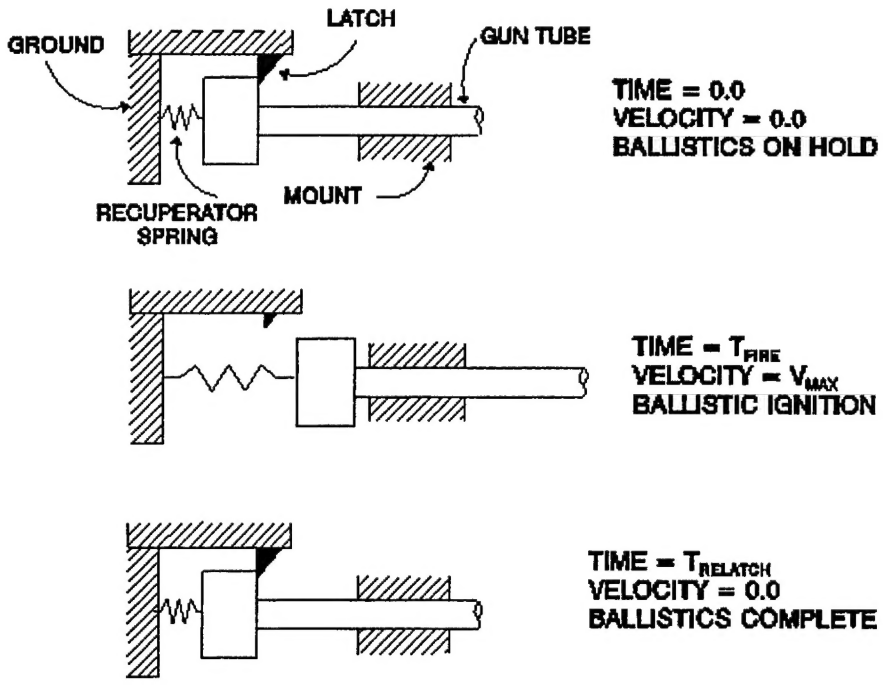

Figure 2. Schematic of a soft-recoil FOOB system.

Energy dissipation is not required for this application; therefore, recoil brakes are not needed. If safety were not an issue, this would be advisable, however, this is never the case. FOOB requires that the ballistic pulse be timed to the dynamics of the forward-moving recoiling parts. If the pulse were applied too early, the required velocity would not be achieved and the rearward stroke of the gun would pass the out-of-battery position by a considerable amount, possibly damaging the mount and support structure. Conversely, if the pulse were applied too late, the gun's maximum recoil would be short of the latch position, thus it would be propelled forward after pressure blowdown impacting the mount in the forward position (normally the in-battery position for conventional operation). The worst scenario is termed a "hang-fire." A "hang-fire" occurs when the shot pulse is applied so late that the forward-moving gun comes to rest as it imparts a heavy load to the mount. Subsequently, the gun fires and it recoils considerably past the out-of-battery position, thus generating additional high forces in the opposite direction. Loads of considerable magnitude would be transferred to the support structure and probably destroy the gun. For these reasons safety is essential in a FOOB gun system.

Description of the M35 Conventional Recoil System

The recoil system used on the 105-mm M35 gun is a generic hydropneumatic, separate system. The brakes and recuperators act independently of each other without a fluid exchange between the two components. The brake components use hydraulic fluid as the medium for energy dissipation, and the recuperators use nitrogen gas as the medium for energy storage. A replenisher attached to the brakes provides additional fluid capacity in the event of leaks or

thermal expansion/compression. The replenisher is connected to the brakes through a small capillary tube, which is designed to operate under static conditions (i.e., when the weapon is stationary). The M35 gun employs two recoil brakes and two recuperators. A photograph of the M35 gun showing the upper units is illustrated in Figure 3. Call-outs indicate the locations for the brakes and recuperators. The brakes are diametrically opposed, as are the recuperators. The components are arranged in this manner in order to minimize vibration-inducing moments about the gun's axial center line. That is, since both brakes and recuperators are concentric with respect to the axial centroid of the recoil mass, the net moment produced by the load buildup in either unit is canceled. This is considered to be an accuracy-enhancing feature.

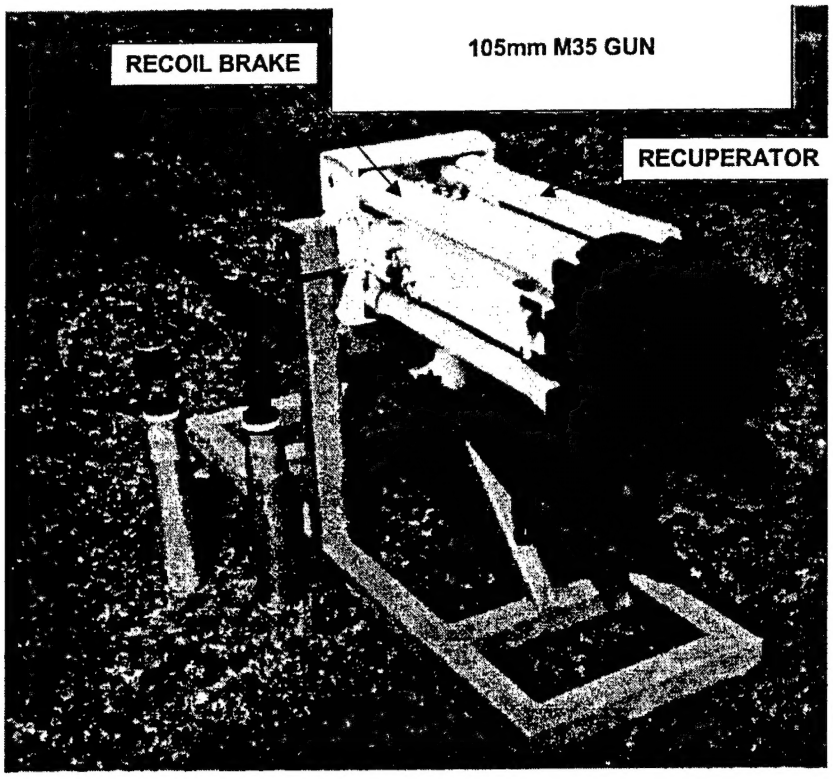

Figure 3. 105-mm M35 gun system.

A schematic of a brake unit in its static configuration is shown in Figure 4. Included in this schematic are the main components of the brake, which are cylinder, recoil rod, control rod, buffer valve, orifice, and end caps. Hydraulic fluid completely fills the internal volume. As shown, the cylinder is attached to the breech, whereas the recoil rod is attached to the mount.

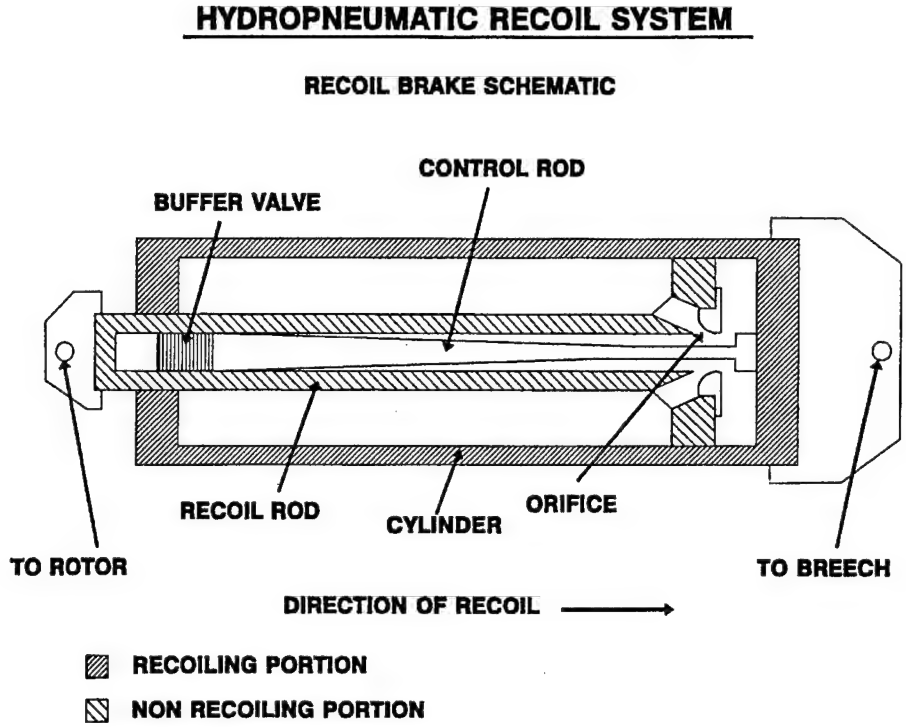

Figure 4. Schematic of M35 recoil brake.

Figures 5a and 5b contain quasi-static views of the recoil brake during operation. The recoil stroke is portrayed in Figure 5a. The recoiling parts include the breech end cap, cylinder, control rod, and buffer valve. The ballistic force drives the recoiling parts to the right, as depicted in the figure. The fluid driven by this motion is squeezed through the annular opening between the control rod and the orifice. Due to the ratio of areas (i.e., annular chamber versus annular through the orifice), the fluid's speed is greatly increased (conservation of mass for incompressible fluid), thus causing pressure increase on the upstream side of the flow. Bernoulli's energy equation is used to model the relationship between pressure and flow speed. (Consult Reference 2 for details of the fluid mechanics involved in recoil brake analysis.) The control rod is profiled such that the pressure distribution in the annular chamber remains relatively constant as the brake extends to its fully recoiled position. Concurrently, a portion of the fluid is driven to the left over the buffer valve into the buffer chamber of the recoil rod. The sizing of the flow path between the buffer valve and the inner diameter of the recoil rod is engineered to accommodate the flow of enough fluid to decelerate the gun during the final portion of the counterrecoil stroke.

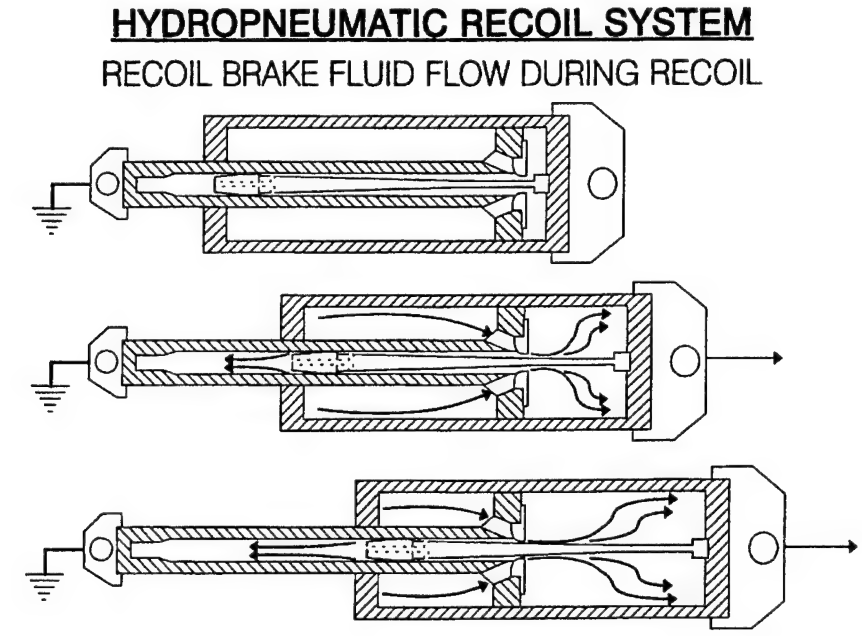

Figure 5a. Fluid flow in brake during recoil.

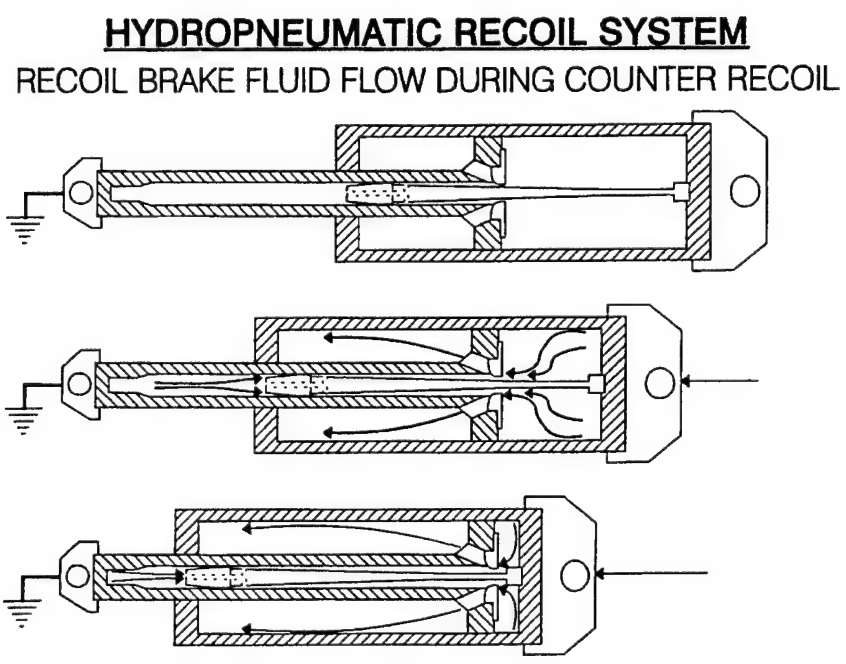

Figure 5b. Fluid flow in brake during counterrecoil.

The counterrecoil stroke is depicted in Figure 5b. During its return to battery from its fully extended position, a reversal in flow direction occurs. Initially, however, there is a void of fluid within the brake, and during the first few inches of counterrecoil motion, the gun accelerates freely. After this void collapses, fluid begins to flow from the front chamber back into the annular chamber through the annular opening between the orifice and control rod. Speeds, however, are relatively slow, and the pressure increase in the front chamber is modest compared to the back pressure achieved in the annular chamber during recoil. Subsequently, the fluid in the buffer pocket begins to flow when the buffer plug reaches this fluid level. The flow path around the plug is annular with several circumferential slots serving as energy dissipaters, thus causing significant pressure increase in this chamber for a modest flow rate. The flats and tapers serve to smooth the pressure distribution such that a relatively constant force is applied to the gun as the valve completes its insertion into the pocket.

Figure 6 contains a schematic of the M35 recuperator unit in its static position. The working medium in this unit is nitrogen gas. It completely fills all available space within the cylinder and inner rod. Ports in the inner rod allow communication between gas chambers. The gas containment system is unique in that it employs a fluid as the seal medium. The two floating pistons (one on the piston head of the inner rod, the other on the cylinder) encapsulate a fluid or grease, and essentially contain the nitrogen completely within the unit. In its static state, this unit is preloaded to several hundred pounds per square inch (psi). This is required to maintain the gun in its firing position for conventional operation at elevation, as well as to "drive" the gun back to this position during the counterrecoil phase of operation.

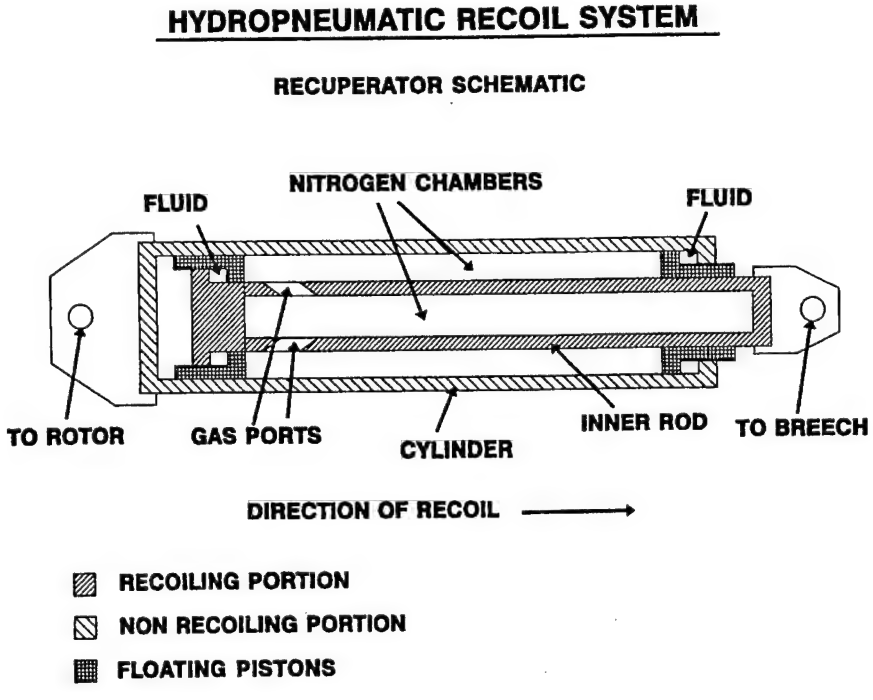

Figure 6. Schematic of M35 recuperator.

The recoil and counterrecoil quasi-static views of the unit operating during recoil and counterrecoil are shown in Figures 7a and 7b, respectively. As the gun recoils, the inner rod and its attached components move to the right with respect to the cylinder and its attached components. The annular chamber volume between the inner rod and cylinder decreases, which compresses the gas, thus increasing its pressure (an isotropic gas law is used to calculate the pressure response). These events are depicted in Figure 7a. When fully extended at the end of the recoil stroke, enough energy has been stored to return the gun to its firing position. Upon decompression, the stored energy is released causing the recoiling parts to be accelerated and returned to their in-battery position. These events are depicted in Figure 7b. The gas volume within the inner rod is essentially a fixed volume, whereas the volume between the rod and cylinder varies as a function of recoil travel. The unit's compression ratio and travel-dependent pressure response are calculated based upon the values of these two volumes. This design feature can be tailored to accommodate various force/travel distributions.

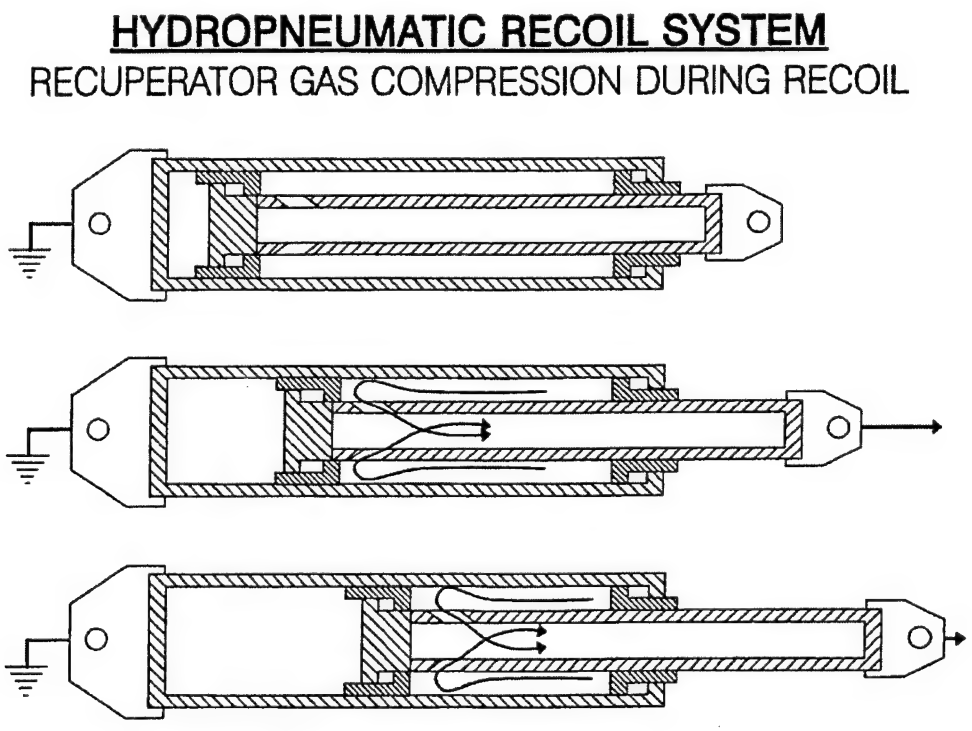

Figure 7a. Gas compression in recuperator during recoil.

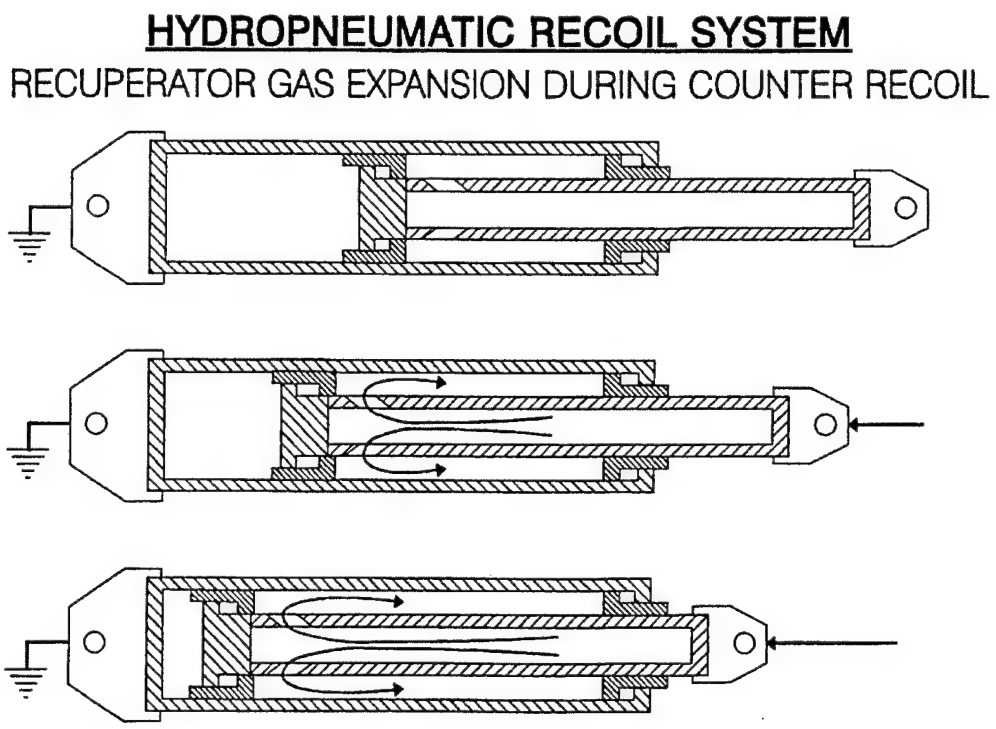

Figure 7b. Gas decompression in recuperator during counterrecoil.

Description of the Modifications for FOOB Testing

Figure 8 illustrates a schematic of the recoil brake used for the M35 FOOB application. It looks similar to the conventional brake shown earlier, with the exception of a long "free-run" area depicted on the control rod as a constant diameter section, as well as a longer buffer valve. Whenever the cylinder's position is such that the "free-run" portion of the control rod is presented to the orifice, hydraulic forces are very low. This is due to the large area through which the fluid flows. Pressure buildup is minimal and provides little retardation to the gun. The buffing profile resides to the left of the "free-run" length and to the right of the buffer valve. When this portion of the control rod passes through the orifice, the area through which the fluid flows becomes restricted. Flow is metered and pressure in the annular chamber increases to provide a retarding force to the recoiling cannon. This area will be activated whenever the gun recoils past its latch position, usually when a premature ignition or a hang-fire occurs. For this FOOB design, the buffing length is four and one-half inches. The counterrecoil buffer valve is four and one-half inches in length, also. Whenever ballistic ignition is later than expected or a misfire occurs, the buffer valve will engage the buffer pocket. Fluid flow from the pocket around this valve will be metered and pressure will build in the pocket. Counterrecoil forces will rise and the gun's velocity in the counterrecoil direction will be controlled. As an additional safety feature, in the event of a misfire, commercial external snubbers (not shown in schematic) acting in parallel with the internal buffers are installed.

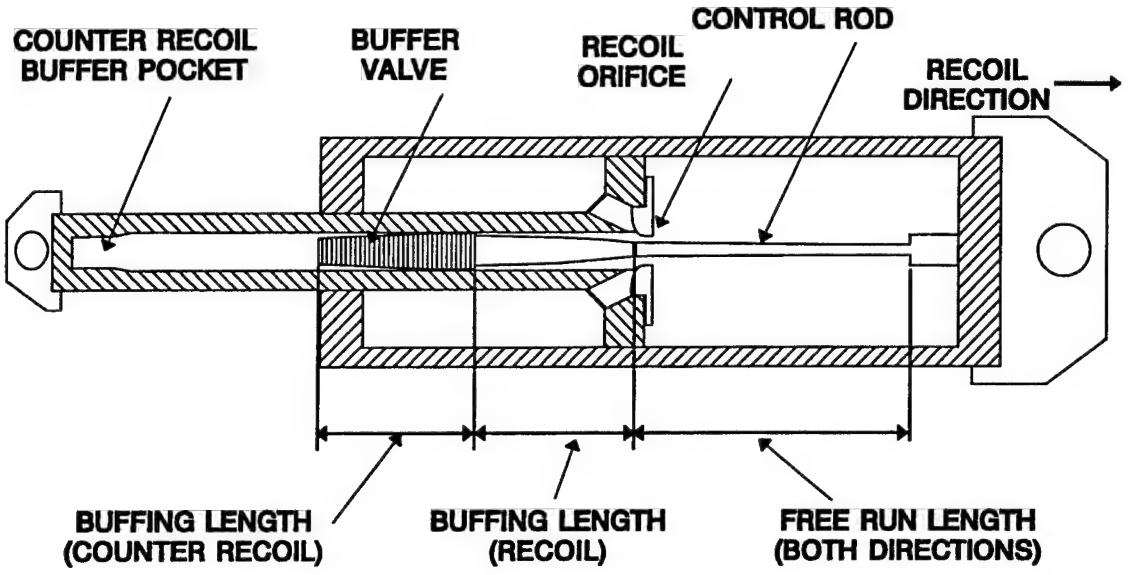

Figure 8. M35 brake schematic for soft-recoil operation.

Detailed comparisons of the fluid flow area in both recoil and counterrecoil are shown in Figures 9 and 10. In Figure 9a, plots of the control rod profile, which is directly proportional to the annular flow area, for both the conventional and FOOB brakes are compared via a diameter versus axial location graph. For the conventional system, the minimum rod diameter is 0.65-inch, which occurs for the first 2.25 inches of recoil travel. This feature provides for low force buildup during projectile in-bore time, and is known to be an accuracy-enhancing feature. From this point, the profile changes rapidly to 0.975-inch. The profile gradually increases to its maximum value of 1.126 inches at 22 inches. The shape of the rod profile may be approximated by piecewise continuous low-order polynomials. The conventional brake provides continuous application of retarding forces from the 2.25-inch position up to the fully extended portion of the recoil stroke. For the FOOB system, the rod profile is dramatically different, as indicated on the second plot of this graph. The minimum diameter of this rod is 0.75-inch and occurs for the first 18 inches of recoil. Since the forces that may be induced on the head of the buffer valve during run-up for a misfire incident are higher for this system than for the conventional system, the buckling characteristics of the rod were considered in this design. Hence, the 0.75-inch minimum diameter was chosen. The "free-run" length extends to 18 inches, after which the rod diameter increases to 1.030 inches, and then gradually increases to 1.126 inches at 22 inches. The rate of change in the diameter is greater for this rod than for the rod used on the conventional brake. In figure 9b, the last 4 inches of the two rods are shown with the axis representing the diameter appropriately scaled.

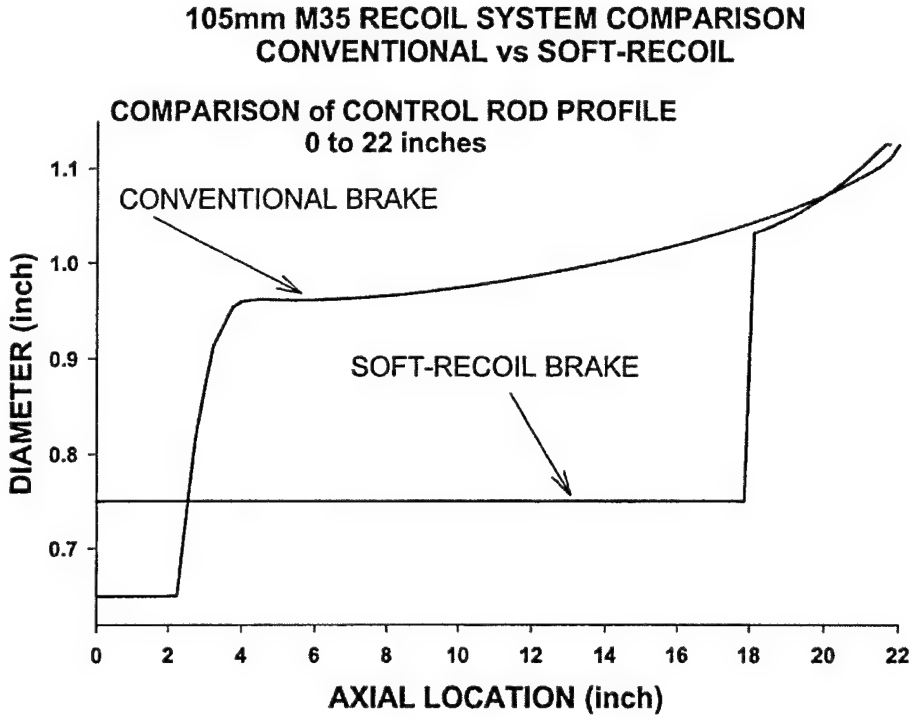

Figure 9a. M35 comparison of control rod profiles (full length of stroke).

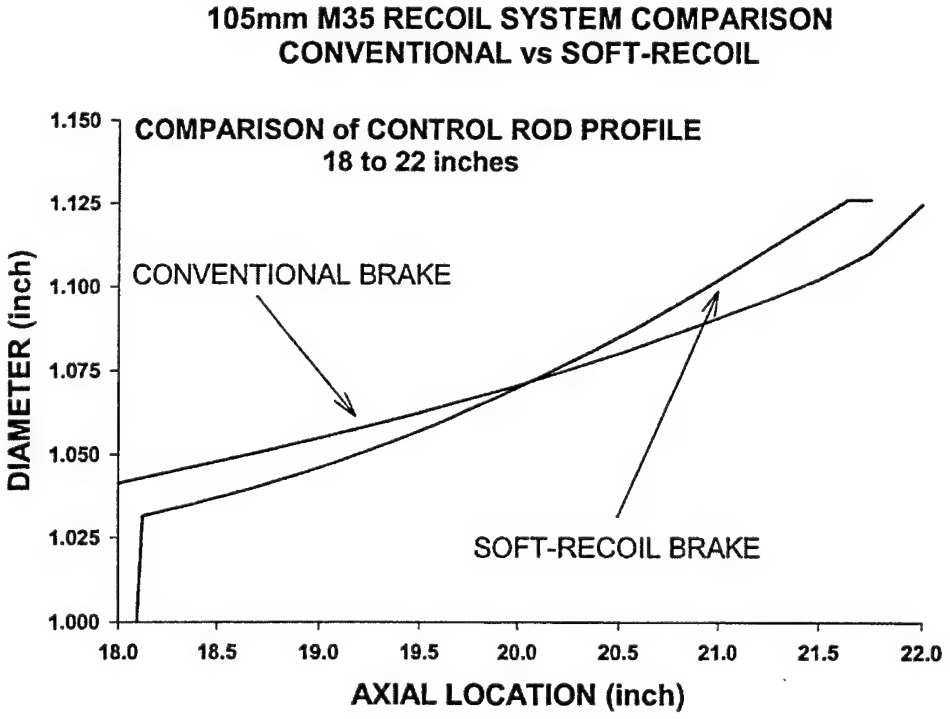

Figure 9b. M35 comparison of control rod profiles (last 4 inches of stroke).

Figures 10a and 10b show a comparison of the restricted flow areas in counterrecoil for the two brake systems. These flow areas are the effective annular areas between the outer diameter of the buffer valve and the inner diameter of the buffer pocket, as the buffer valve intrudes into the buffer pocket. Since the buffer valve has a tapered outer profile and the buffer pocket is of constant diameter, the effective area is an average area based upon the total volume between the two parts and the insertion depth of the valve. Since the restricted flow path has some length, the viscosity of the fluid contributes to the pressure rise in the buffer pocket. As shown in Figure 10a, the area is quite small for both designs for the last 2.5 inches of counterrecoil travel (this graph must be read backward, i.e., at zero axial location the gun is at its in-battery position). At 2.5 inches, this area opens up for the conventional system. For the FOOB system, this area does not open up until the gun is 4.5 inches from in-battery position. Rearward of these two locations, the effective area increases significantly offering no resistance to fluid flow essentially eliminating back pressure and providing no opposing force to the forward accelerating gun. Figure 10b depicts the flow areas for the final 5 inches of counterrecoil travel. For the conventional brake, this area closes rapidly, as indicated by the discontinuous slope in the plot. These discontinuities are representative of the discrete changes in diameter along the axis of the buffer valve. For the conventional brake, there are two steps; whereas, the other brake has only one. The counterrecoil flow area for the FOOB brake begins to close at 4.5 inches from in-battery position and is reduced at a much slower rate. The discontinuity in slope at 1.5 inches represents the step change in the valve's diameter.

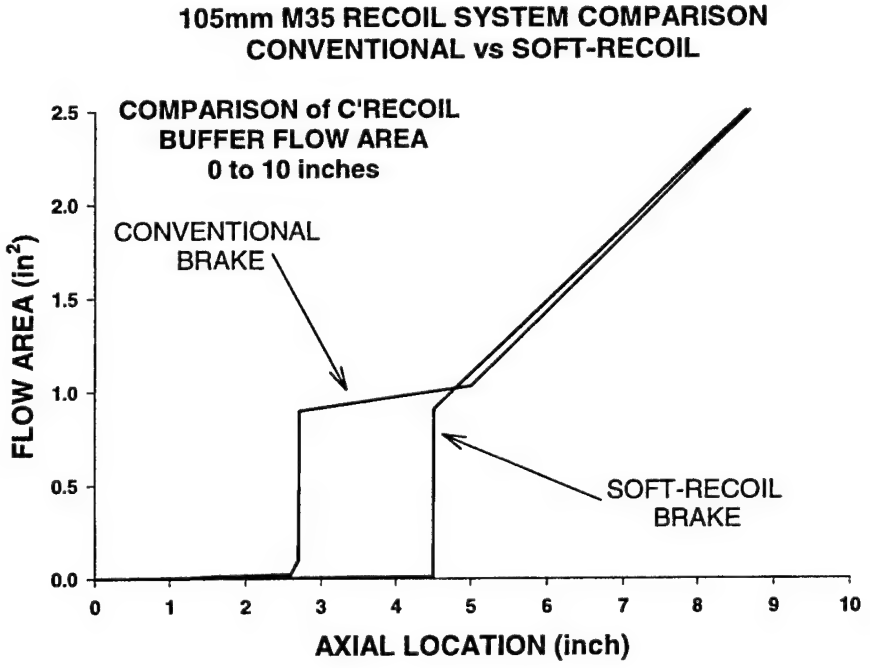

Figure 10a. M35 comparison of buffer flow areas (0 to 10 inches travel).

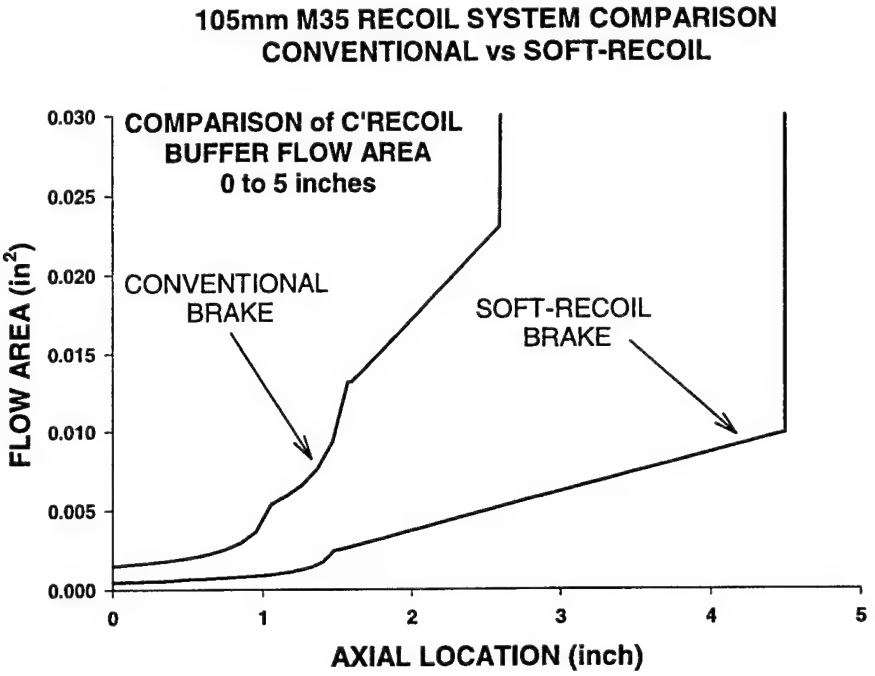

Figure 10b. M35 comparison of buffer flow areas (0 to 5 inches travel).

Through a series of schematics and some technical discussion, the functions of both a conventional and FOOB recoil system have been explained. The next section will highlight the results of firing the conventional M35 gun system using a low impulse (M724) round. The need for such firings and the use of the data collected from the tests will be explained.

BASELINE TEST FOR M724 ROUND

Rationale for Test

Successful operation of a FOOB system requires that the ballistic pulse be timed to the kinematics of the forward-moving recoiling parts. If the pulse were applied too early, the required velocity would not be achieved, and on the rearward stroke, the gun would pass the latch position and possibly damage the weapon. Conversely, if the pulse were applied too late, the gun would not recoil far enough to relatch, thus it would be propelled forward after pressure blowdown impacting the mount in the forward position. In the ballistics world, it is universally known that the ignition process for service rounds using standard granular propellant inherently contains some timing uncertainty. This uncertainty manifests itself as delays in the initiation of pressure rise, pressure peaks, and blowdown. The delays are an artifact of the ignition process and its flame spread mechanism that is stochastic in nature.

Based upon a study of transient recoil responses for early versions of the M35 gun (circa 1989) (ref 3), this uncertainty may be as much as 5 milliseconds depending upon round type and lot number. Baseline testing prior to a full-scale FOOB demonstration is required to reconfirm the ballistic uncertainty and determine the exact value of the charge impulse. This must be accomplished as early as possible, since follow-on simulations using Benet's recoil analysis codes will be used to determine the optimum ignition time and the location of the firing trigger switch.

Establishment of Ignition Delay

For FOOB application the initiation of the shot pulse is paramount to successful operation of the weapon; therefore, an assessment of the ignition delay times for the M724 round became part of the baseline test. In tests performed in the late 1980s (ref 3), the initiation of recoil travel was used to determine the shot delay time for both HEAT and kinetic energy rounds. Although this is a reasonable measure of ignition delay, the acceleration response of a component within the weapon would be a better indicator. Acceleration responses that appear before any discernible movement are of much higher magnitude and instantaneously applied, therefore their presence is easily detected and recordable. Moreover, the delay time that is needed is the difference between the application of the voltage to the firing circuit and the initial activity in the chamber. For the baseline test, we measured four responses directed at resolving the timing-delay issue; namely, voltage and current in the firing circuit, axial acceleration on the breechblock and breech ring. Upon initial inspection of the raw data for all shots in this test, it was determined that only the voltage response and breechblock acceleration were needed. In fact, the acceleration signals in the breechblock and ring occurred simultaneously, whereas the lag time between voltage and current was relatively constant for all shots in this test.

Ten shots were fired in this baseline test and usable data for timing assessment was recorded as transient plots of firing voltage (V) and axial acceleration (g's) versus time. Since the characteristic response for all ten shots was the same, the transient response for only one shot will be presented and discussed in this portion of the report. The results are shown in Figures 11 and 12. Figure 11 contains the voltage plot for shot #1 in two time windows; namely, 50 milliseconds (ms) and 2.5 ms. By examining the results in the larger time window depicted in the leftmost plot, the initiation of voltage response is easily discernable. It resembles a step function rising from 0 to 28 volts at approximately 26 ms after the time zero signal. The voltage "settles" and remains at 28 V for about 10 ms and then oscillates slightly for the remainder of the event. This oscillation is due to electrical interference from the accelerometer circuits, since it is at this point in time (i.e., ~36 ms) that the accelerometer begins to respond. (This will be discussed later.) The other plot on the right shows the local structure of the response in a much smaller time window. It is slightly oscillatory in nature in that two complete cycles ranging from 15 to 29 volts are indicated. This structure is not unusual for step-like inputs. Unless the circuit is highly damped, a step-function input will overshoot its target and then oscillate for a few periods until it levels off.

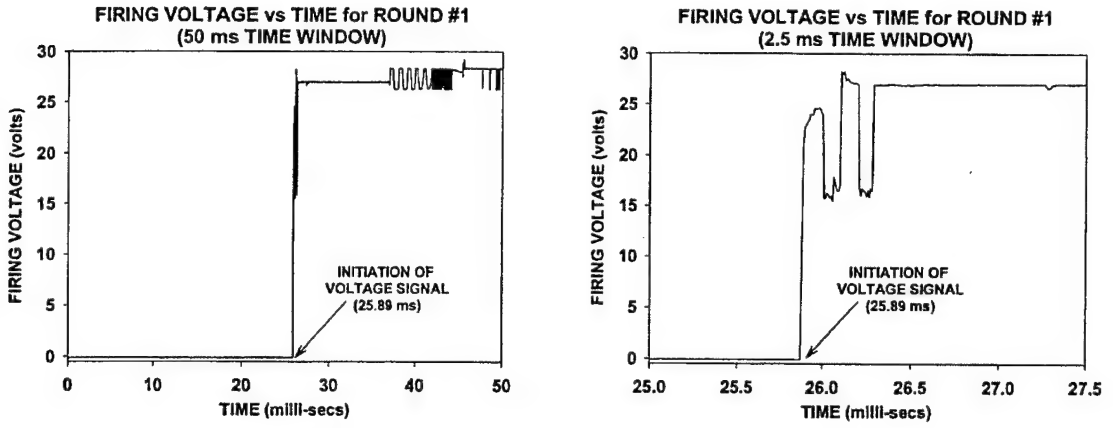

Figure 11. Firing circuit response for round #1.

Block acceleration, however, is another issue. It does not respond as a step function, rather it presents itself as a harmonic wave the initiation of which is highly subjective. Due to the saturation level at which the response circuit was set (±10 g's), it appears that much of the data were not recorded. In normal recoil, the M35 achieves over 300 g's; therefore, by limiting the collection level to 10 g's, the early portion of the response would be magnified, whereas the remaining would be saturated. This was fine for the test being conducted. Our goal was to determine the initiation of ballistic activity by examining the dynamic response of the breechblock during pressure buildup.

Figure 12 contains the acceleration plot for shot #1 in two time ranges; namely, 50 and 4.0 ms. In the 50-ms plot shown on the left, four significant areas of response are shown. First, short time duration "spikes" about 26 ms are shown. Since this time coincides with the application of the voltage pulse (see above), this signal is merely electrical interference from the voltage circuit. About 10 ms thereafter, a low-frequency, low-amplitude signal develops. This represents primer actuation and initial loading of the breechblock. The direction is always the same, namely negative. A few ms later, a saturated oscillatory higher-frequency response is shown. This is due to the "ringing" of the block within the breech ring before any discernible ballistic pressure has been achieved. Somewhat later at 41 ms, a unidirectional saturated response in the negative direction is shown. This is due to the high ballistic force that "holds" the block against the mating portion of the breech ring, while the entire gun accelerates rearward as a rigid body. The area of most interest is the initiation point of the signal. In the other plot at the right, a 4-ms window is shown centered at the point of initial activity. Although the actual location is subjective in nature, the signature of this portion of the data is the same on all shots. For this first shot the "initiation time" was determined to be 33.54 ms.

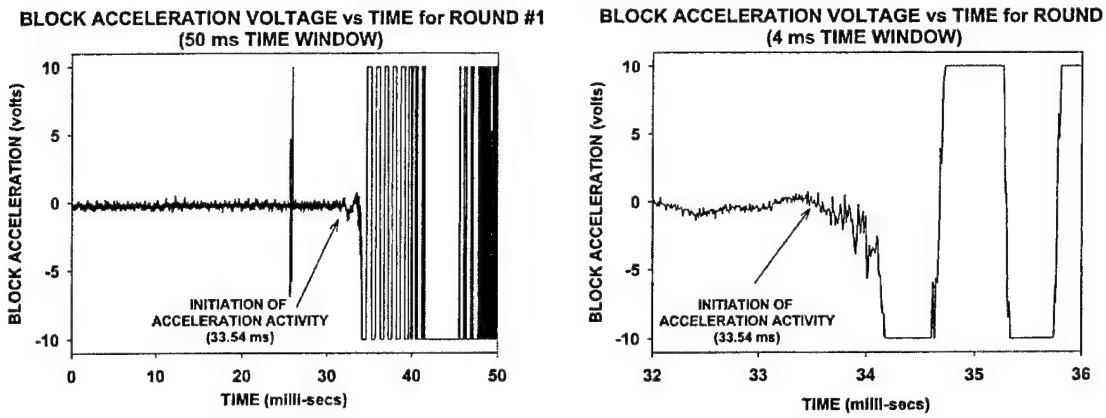

Figure 12. Block acceleration activity for round #1.

Reiterating, the purpose of this portion of the test was to determine the delay time between application of the firing voltage and the initiation of ballistic pressure in the breech. Figures 13 and 14 show the results of these determinations for all ten shots. Figure 13 contains the time at which voltage application occurred (normally oriented triangles) and the time at which acceleration activity was detected (inverted triangles). As shown, voltage application times were very repeatable (mean = 25.67 ms; std. dev. = 0.21 ms), whereas occurrence of acceleration was not (mean = 35.48 ms; std. dev. = 1.52 ms). By subtracting comparable pairs of values (i.e., acceleration time minus voltage time for a given shot), we arrive at the delay time for each. This is the important value needed for a FOOB application. Delay time results are shown in Figure 14 along with the statistical values for all ten shots. The mean value was 9.81 ms, whereas the standard deviation was 1.54 ms. These values will be used in a subsequent simulation to determine at what point in the run-up stroke the firing circuit must be activated such that the recoiling parts return to the latch position and re-engage.

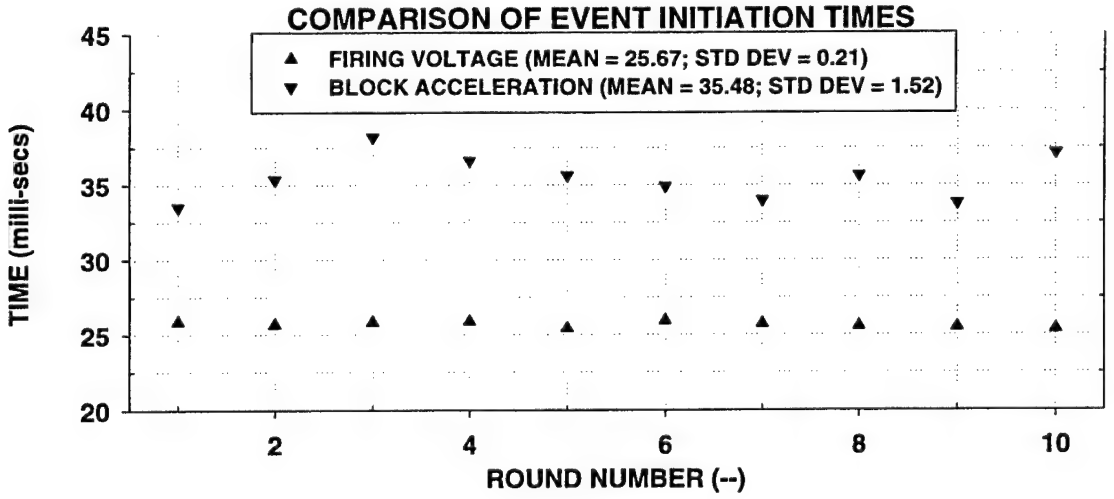

Figure 13. Comparison of electrical versus mechanical signal initiation for all rounds.

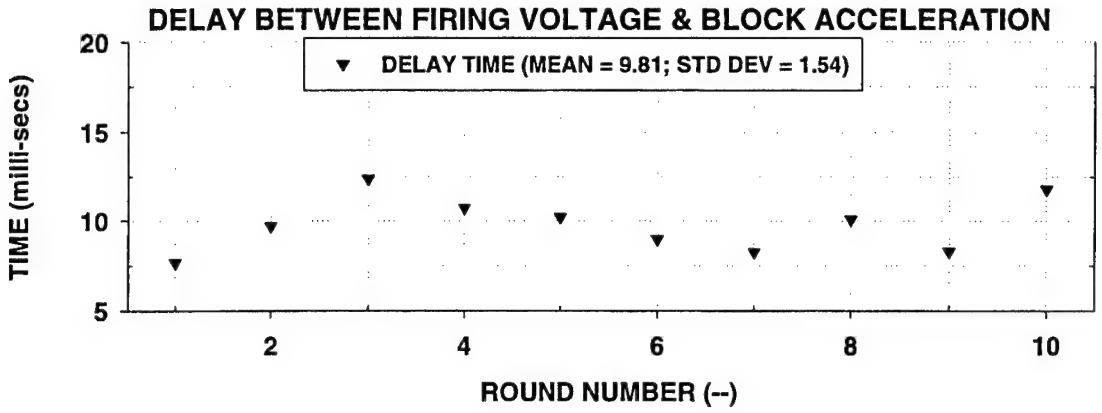

Figure 14. Delay time calculation of signal initiation for all rounds.

Determination of System Responses

This portion of the test consisted of firing six M724 rounds and collecting time-dependent recoil system data for each shot; namely, pressure in both brakes and one recuperator, forces through load bars that are located between the mount and trunnions, travel by using the Temposonic device, and muzzle velocity using standard Wright-Malta Corporation (WMC) procedures. In addition, the data recording software (VuePoint[8]) was programmed to calculate recoil velocity from the position data. As with the voltage and acceleration data, the transient responses for one shot (shot #2) will be presented and discussed in detail. With very few exceptions, the data for all six shots behaved similarly. Time zero for the data has been adjusted based upon the timing results discussed in the last section.

Figure 15 shows a summation of trunnion force data for shot #2. A considerable amount of information may be acquired by examining this plot. As shown, the trunnion force starts from zero and quickly rises in about 0.010-sec, after which a slight oscillatory response is indicated. This is due to the elastic nature of the load-bar material. A peak force of 35 kilo-pounds (kips) occurs at 0.020-sec after which the force level decreases to a constant level of 10 kips at 0.100-sec. The knee in the force curve indicates that the gun is fully recoiled and ready to return to its in-battery position. The force response during the initial portion of the cycle (i.e., up to 0.100-sec) is mostly due to the hydraulic pressure in the two brake cylinders. When the gun is momentarily arrested in full recoil, brake pressure drops to zero and the remaining force is wholly due to the gas pressure in the recuperators. This is indicated by the long-duration, fairly-level response from 0.100-sec to about 0.175-sec. Although the gun is returning to its in-battery position during this time, the brakes are not providing any resistance due to the increase in air volume resulting from an extension of the cylinder and rod. (Note: when a brake extends, a void is created in that there is more available air volume than fluid volume.) At 0.175-sec, this "void" closes and fluid begins to flow back across the main orifice, inducing braking force in the counterrecoil direction. This event occurs quickly, thus a negative force "spike" occurs. Braking force is now being provided in the reverse direction until such a time (about 0.250-sec) when the brake and recuperator forces are equal and opposite, thus a net force of zero is shown.

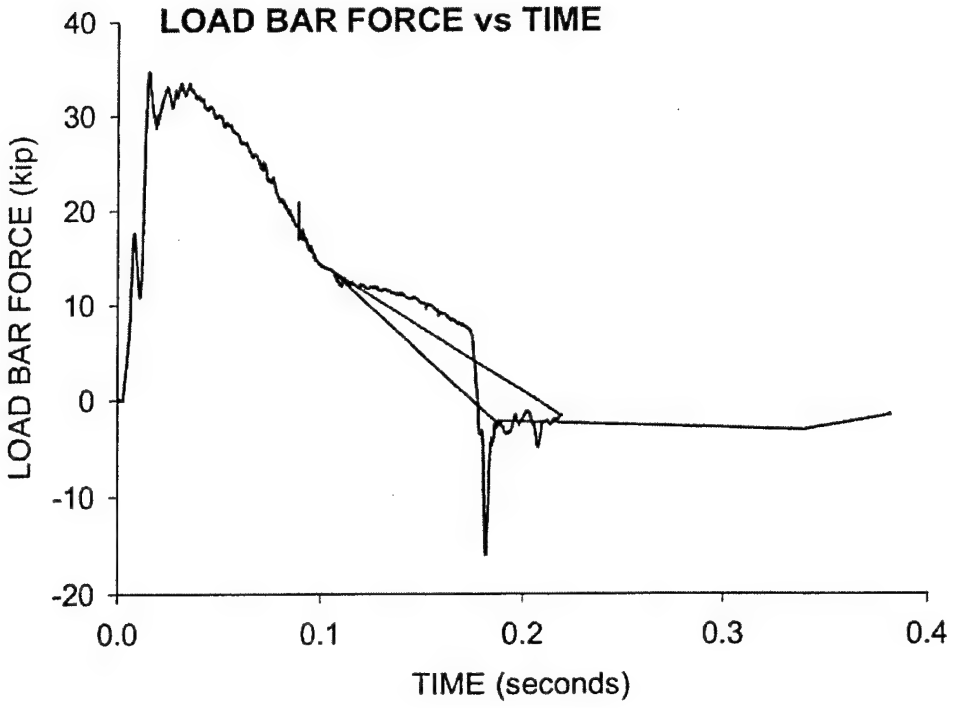

Figure 15. Trunnion force versus time for round #2 baseline test.

At 0.300-sec the counterrecoil buffer plug engages its mating buffer chamber, thus initiating restricted flow from this pocket and providing an additional retarding force. Much like the commencement of reverse flow in the main orifice, the initiation of flow from here is instantaneous, so a force "spike" is indicated. The forward speed of the gun is reduced until the buffer plug becomes deeply inserted into the pocket, at which time another force "spike' is indicated at 0.400-sec. (The M35 gun used for this test was an early model in which the counterrecoil buffer design was not optimized. This was addressed in subsequent iterations, yielding a return force distribution that is much smoother.) The entire recoil-counterrecoil cycle consumes 0.400-sec. The integration of this force data from the beginning of the recoil stroke, until it achieves a fully recoiled position, is the impulse delivered to the system. This is a direct measure of the impulse in the charge and was used to determine its value.

Figure 16 depicts the total force in the brakes during the recoil portion of the cycle. This plot contains the summation of the force output from both brakes. These data were derived from the measured pressure in the recoil cylinders multiplied by the piston area. The individual plots for each brake were nearly the same. Unlike the load-bar data, this signal does not indicate a low-frequency oscillation; however, a low-amplitude, high-frequency disturbance due to wave motion in the fluid is shown for much of the response. This is a characteristic response for all fluid braking systems and is of little concern regarding a brake's performance. The brake force rises at the same rate as the load-bar data (~0.100-sec), then ramps down to zero at 0.100-sec. Since the pressure gages are located in the brake cylinder, the force buildup during counterrecoil could not be measured, therefore the last 0.300-sec of the plot is essentially zero. It should be noted the "spike" appears just under 0.190-sec. This corresponds to the shock that develops abruptly in the fluid as reverse flow through the orifice commences.

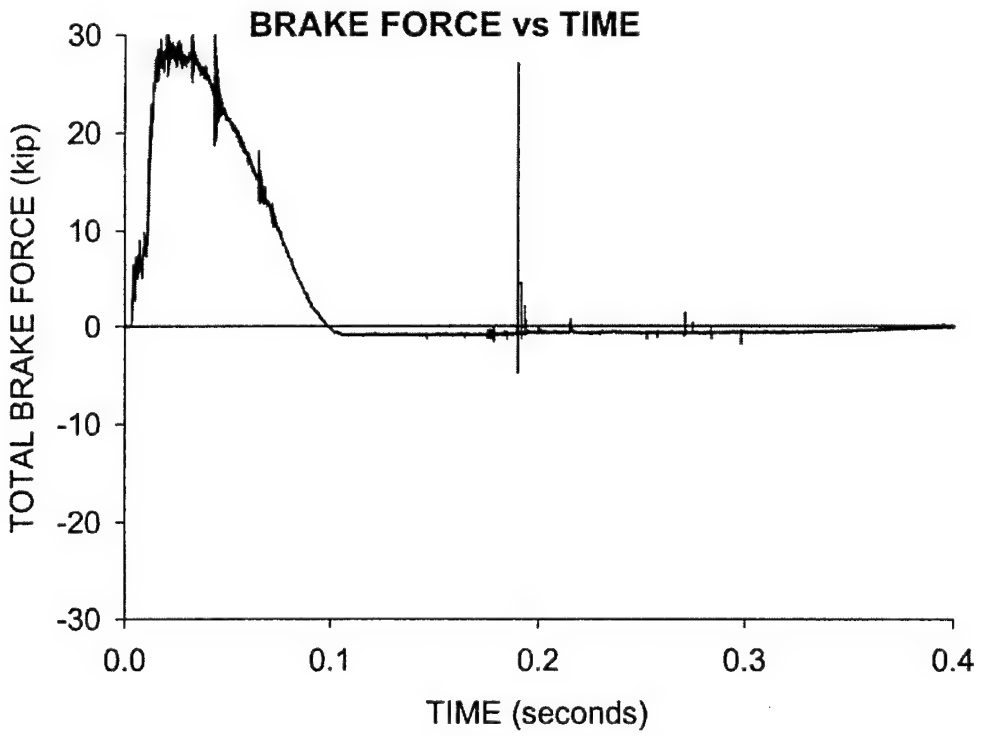

Figure 16. Brake force versus time for round #2 baseline test.

Figure 17 shows total recuperator force. As with the brake force data, these data were derived by converting recuperator pressure to force for each unit and summing both to arrive at the total. The recuperator is just a gas spring, therefore, the force is directly proportional to recoil displacement and the parameters of the nitrogen gas within the unit. Isotropic compression is expected and this response behaves quite well according to theory. The initial force of approximately 4500 lbs is due to the preload on each unit. As the recoiling parts are displaced rearward, the gas compresses, thus increasing the force. At ~0.100-sec when the recoil stroke is fully extended, the force value peaks at ~15,000 lbs. From this point forward, the gas slowly decompresses and "pushes" the recoiling parts back to their in-battery position. This portion of the event takes about 0.300-sec.

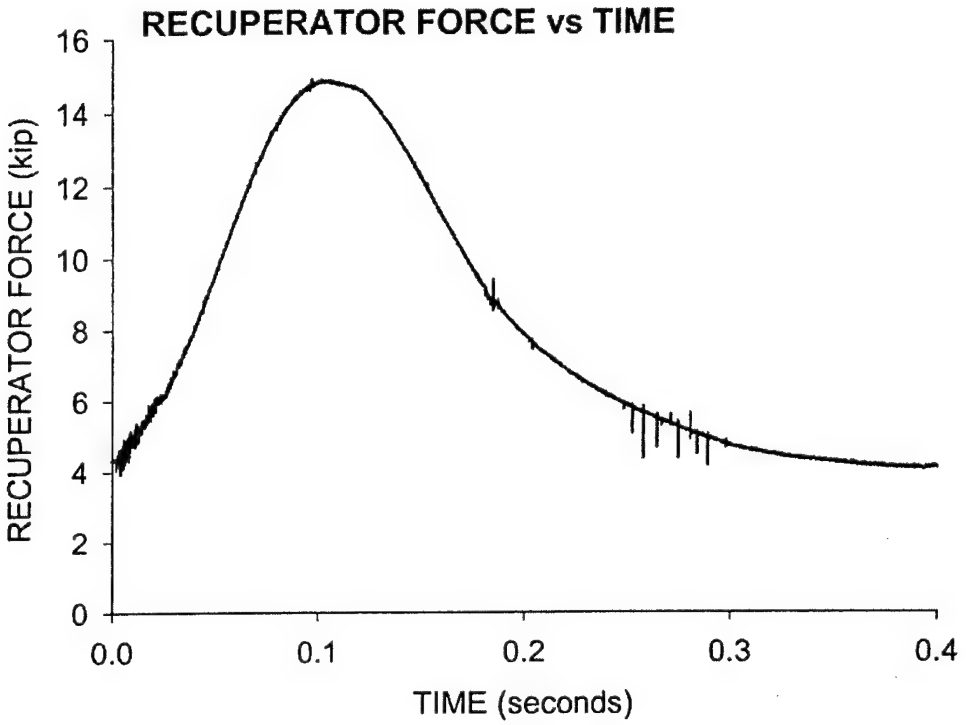

Figure 17. Recuperator force versus time for round #2 baseline test.

Figure 18 depicts the position of the recoil parts versus time. The shape of this response is quite similar to the recuperator force response. A few "blips" appear on this trace just before the gun has achieved full recoil. These are nuances in data acquisition and should be ignored. The gun recoils to its fully extended position of ~20 inches in 0.120-sec and then returns to zero in the last 0.300-sec. The recoil velocity response is shown in Figure 19. This velocity measurement was not direct, but rather derived in VuePoint[8] by a numerical differentiation of the recoil position versus time data. The high-frequency, low-amplitude response on the velocity trace is attributable to the "noisiness" of the displacement data and the numerical differentiation process. (We believe a 20-point averaging of the displacement data was used for smoothing prior to differentiating.) These oscillations are quite severe at 0.075- and 0.090-sec. This may be disregarded in that the "global" response is most important. The recoil direction is indicated by a positive direction and vice versa for counterrecoil. Initially, the velocity rises quite rapidly achieving a level of nearly 350 inches per second (in/sec) at 0.015-sec. It falls at a slower rate finally crossing the time axis at 0.120-sec. The gun's direction is reversed and the velocity returns the gun to its in-battery position. During counterrecoil, the maximum speed achieved is about 130 in/sec that occurs at 0.175-sec. At this time the response abruptly changes slope and begins its descent to zero. This corresponds to the first occurrence of a brake pressure "spike" discussed above. The subsequent "spikes" are not of high enough magnitude to be discernable in the velocity distribution. The response smoothly approaches and returns to zero at ~0.400-sec.

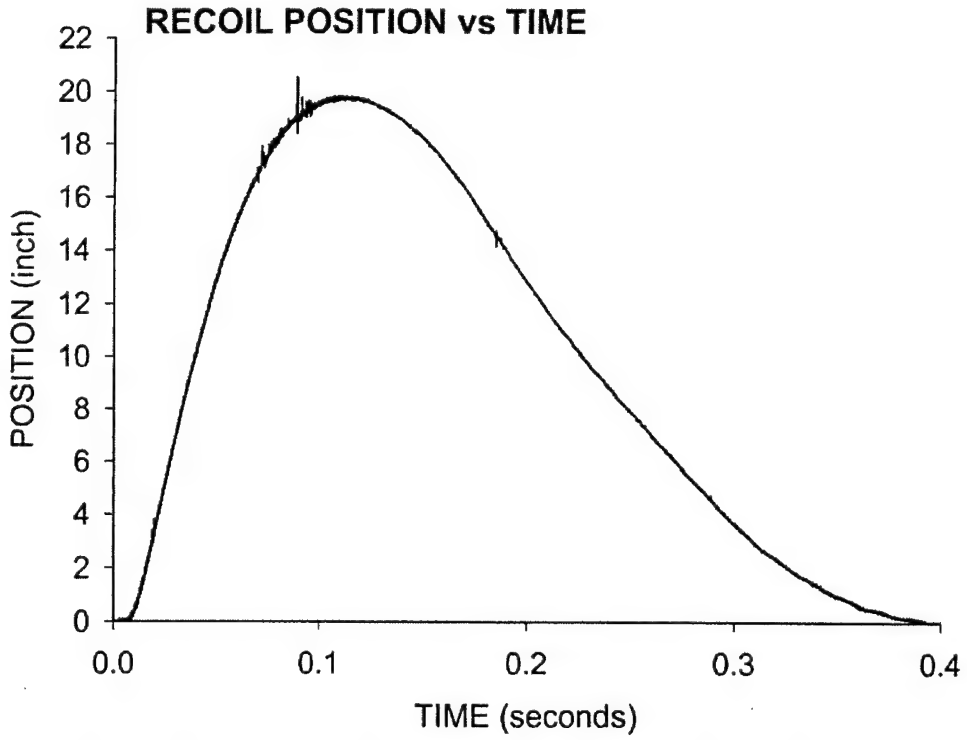

Figure 18. Recoil position versus time for round #2 baseline test.

Since we could not directly measure the ballistic pressure driving the system to determine the impulse levels, the trunnion load data were used. Typical of all mechanical systems, momentum must be conserved. This being the case, momentum changes are manifest in the time integrals of applied loads. In our case, the driving load is the ballistic force on the breech, whereas the reacting load is concentrated through the load bars and applied to the trunnions. Since the gun velocity is zero before ballistic activation and returns to zero when the gun has fully recoiled, the net momentum change is zero. Therefore, the time integrals of the ballistic pulse and the trunnion load must be of equal magnitude. The ballistic impulse, therefore, may be determined by integrating the trunnion reaction load.

Additionally, since we recorded brake and recuperator forces, we may redundantly determine the impulse by integrating these distributions. The only impulse lost from this measure is friction. For the rounds in the test only, the load-bar data were clean enough for all six shots such that an integration could be performed. The time range for the integration begins at the inception of recoil displacement and ends when the rearward velocity ceases. The velocity plots in VuePoint[8] were used to indicate these times. Referring to Figure 19 for shot #2, velocity begins about 0.01-sec and ends at 0.120 -sec. Using these time limits (they were different for each round) for integration, the impulse value for the M724 round was determined to be 2628 lb-sec with a standard deviation of 20 lb-sec and a range of 68 lb-sec. By comparison for shot #4 (for which all brake and recuperator data were clean enough to integrate), the impulse derived by integrating the trunnion force is 2629 lb-sec. The impulse determined by integrating the two brake forces is 1795 lb-sec, and for the two recuperator forces it is 615 lb-sec. The total impulse from these measurements is 2409 lb-sec, which underestimates the trunnion force integral by 220 lb-sec, and is about 8 percent low.

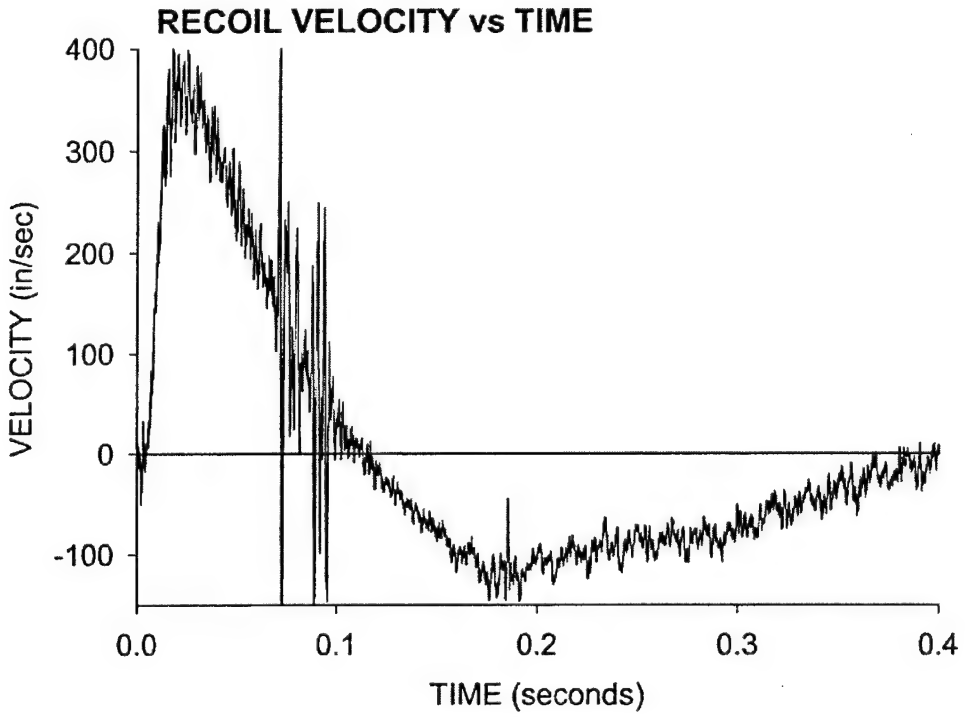

Figure 19. Recoil velocity versus time for round #2 baseline test.

Comparison of System Responses to Simulations

To establish validity of the predictions and subsequent use in developing a timing strategy for FOOB, simulations were conducted and compared to the firing results. Specifically, shot #2 is used for this comparison (although average of all the shots might be a better measure of the system's response tendencies). The results of these comparisons are shown in Figures 20 through 24.

Figure 20 shows the trunnion force data for shot #2 with the predicted response superimposed in a dotted line style. Since the model does not treat the elastic properties of the load bars, the oscillations that are shown in the data could not be predicted; however, the global distributions are qualitatively the same. In the initial portion of the cycle, the predicted response overshoots the data by about ten percent at its maximum level and remains somewhat high for the duration of the recoil cycle. During counterrecoil, which begins at about 0.100-sec, the predicted response and the data track each other quite well until the reverse shock develops its occurrence at 0.190-sec. The timing for the predicted response is early by about 0.010-sec and the range in the reversal is about two-thirds that of the data. This should not be a concern since the measurement transducer is elastic possessing dynamic characteristics, and the measured shock level could be an overshoot of the gage. However, the secondary shock that occurs at 0.300-sec in the predictions and at 0.400-sec in the data is roughly of the same magnitude. This occurs when the buffer plug becomes fully inserted in its mating pocket. In the model (as will be shown later in the travel plot), the arrival time is much quicker than shown in the data and occurs immediately after the low-level step at 0.290-sec.

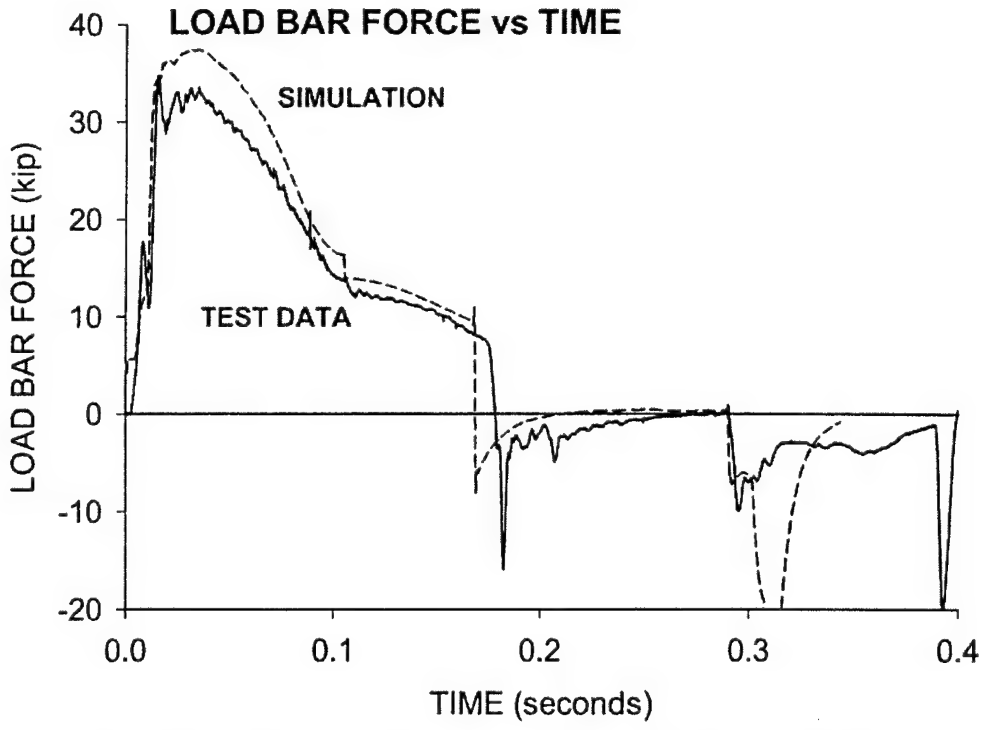

Figure 20. Analytical comparison of trunnion force versus time.

In Figure 21 the data for the brake force is shown with the predicted response superimposed in a dotted line style. The bulk of the trunnion force is due to the brakes' response, therefore, the distribution is same for both. As mentioned earlier, the brake pressure could not be measured during counterrecoil, so the comparison between the predicted value and the data could only be made up to 0.100-sec. During this time, the two track each other quite well with the calculated response just slightly higher than the measured value.

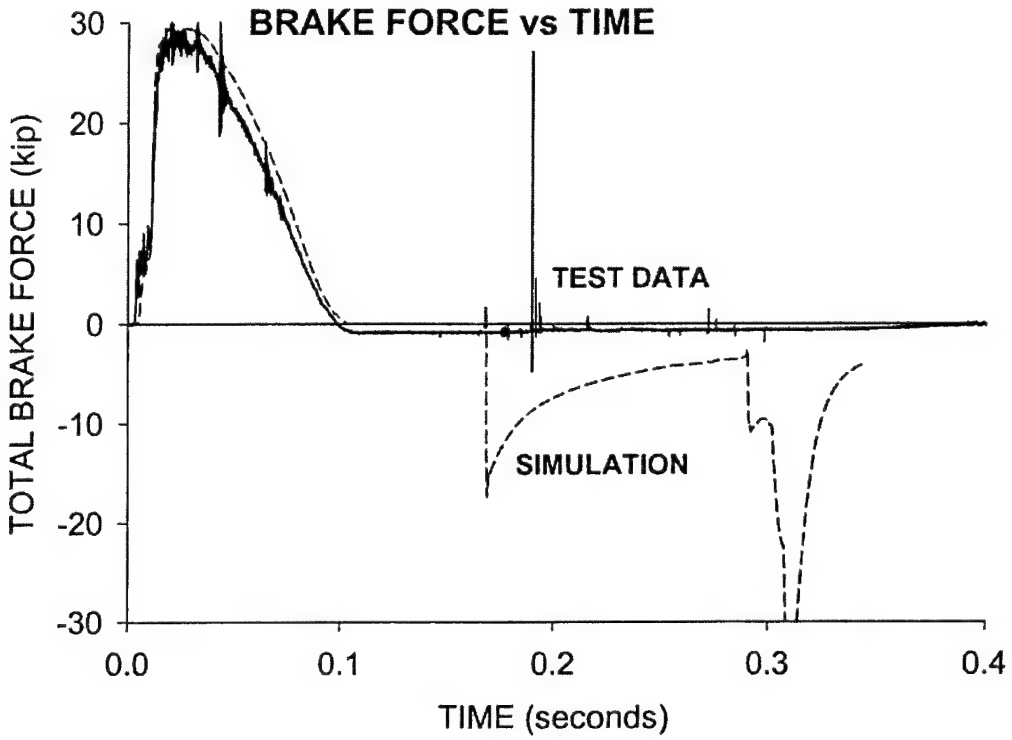

Figure 21. Analytical comparison of brake force versus time.

Figure 22 depicts the data for the recuperator force with the predicted response superimposed in a dotted line style. There is not much to say about this prediction, since both data and prediction track quite well. The recuperator is just a gas spring, its response being a function of displacement only.

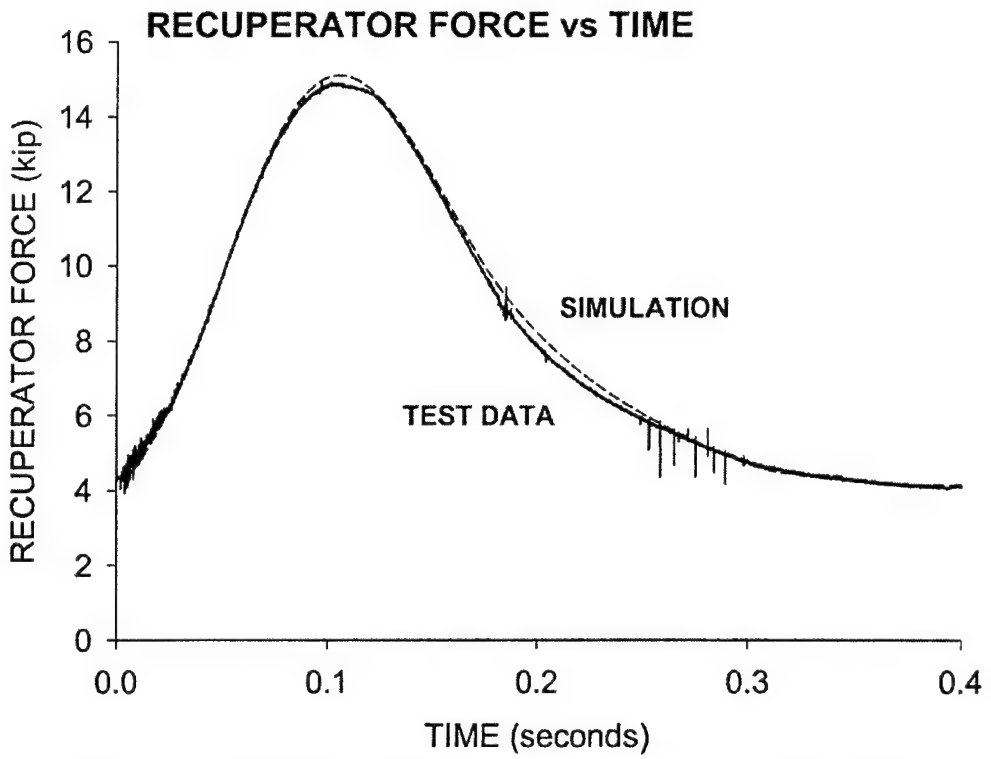

Figure 22. Analytical comparison of recuperator force versus time.

Figure 23 shows the data for the recoil position with the predicted response superimposed in a dotted line style. The shape of each plot is the same; however, the duration for the predicted response is about 0.050-sec shorter than that for the data. However, the peak values occur simultaneously and it is at this point that a crossover of the response occurs. Referring back to the trunnion load response, the predictions indicated that the in-battery position occurs at 0.350-sec, at which time a rather large shock load occurs. For these data, this occurrence is at 0.400-sec.

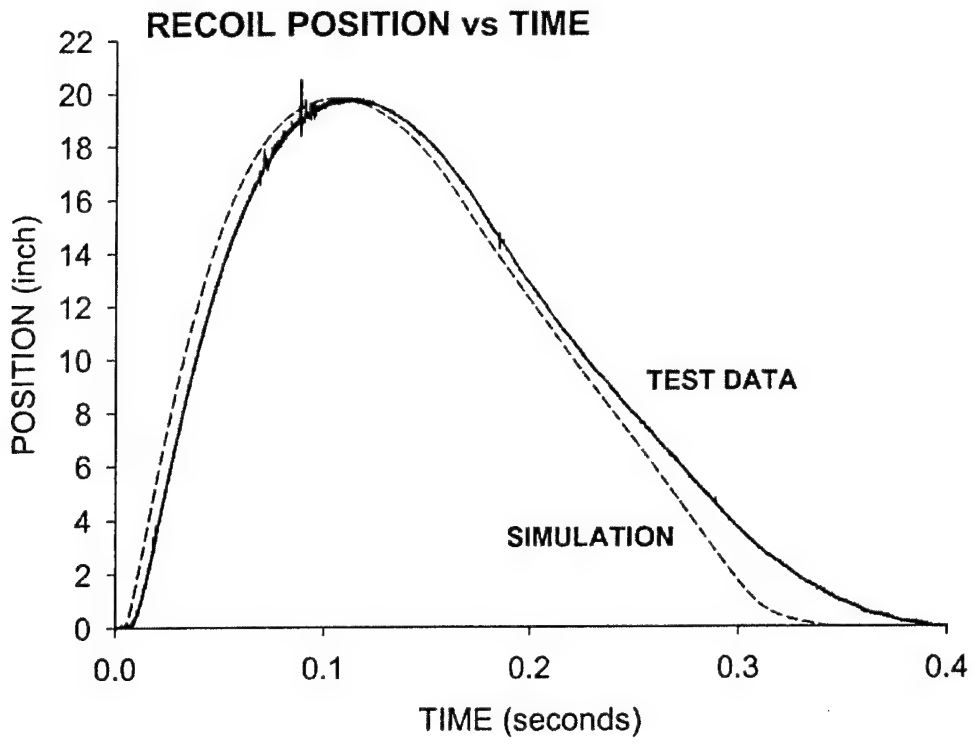

Figure 23. Analytical comparison of recoil position versus time.

Figure 24 records the recoil velocity data for shot #2 with the predicted response superimposed in a dotted line style. Reiterating, the recoil velocity data were derived by a numerical differentiation of the travel data using a smoothing algorithm to decrease "noise" in the calculation. However, as indicated in the data, some "noise" remains. We must compare the overall shape of this response, and in doing so we may conclude that both track each other quite well. The initial rise from the predicted response is quicker than that shown in the data, but the peak values are comparable. The remainder of the response indicates the same tendencies; namely, the point at which the crossover occurs from recoil to counterrecoil (about 0.100-sec), the rapid deceleration at 0.175-sec, and the terminal velocity of about 10 in/sec at 0.350-sec. Again note the timing differences of 0.050-sec at the end of the cycle.

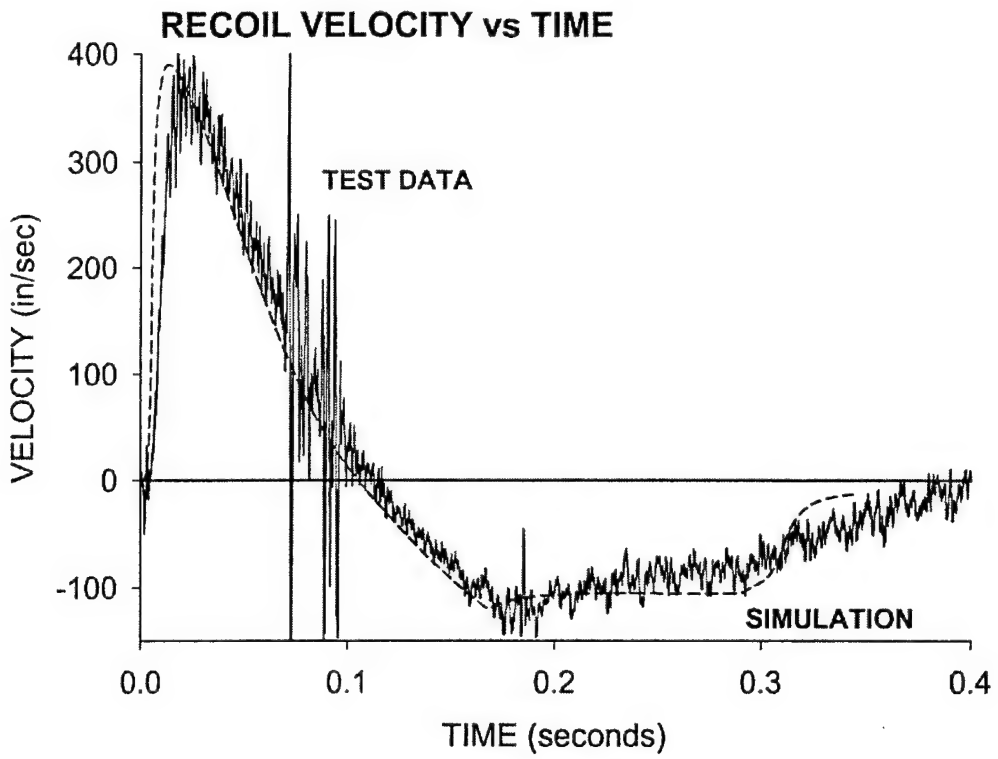

Figure 24. Analytical comparison of recoil velocity versus time.

Considerable information was gained by conducting the M724 baseline test and subsequent simulations. The ignition delay of this round was firmly established. This is paramount to firing the weapon as a FOOB system. Additionally, considerable confidence in the recoil simulation model was achieved by comparing the predictions to the firing data. The results of this test and simulations were used to establish the location of the firing trigger switch for FOOB application. Test and simulation results for the FOOB firings will be presented next.

RUN-UP TEST

Rationale for Test

Reiterating a previously written statement, "Successful operation of a FOOB system requires that the ballistic pulse be timed to the kinematics of the forward-moving recoiling parts." Since the delay time of the charge needs to be accommodated in the firing sequence, it is imperative that the run-up kinematics of the recoiling parts need to be determined such that the location of the triggering mechanism for the firing circuit be appropriately located. Subsequent to the baseline test and prior to FOOB firings, a six-shot run-up test was conducted at the WMC test site using the recoil brakes containing a FOOB-designed control rod, latching system, and two recuperator preload values of 1000 and 2500 psi. It was anticipated that the 2500 psi level would be needed to achieve a run-up speed commensurate with the impulse level of the M724 round. From these test results, this assumption would be confirmed or refuted. The conduction of the test followed a precise sequence of operations. First, the recuperators were deflated and the gun was physically displaced to its latch position (rearward 17 inches). Second, the gun was latched and the recuperators were re-inflated to the desired pressure value. Third, the latch was

released and gun moved forward. The gun's motion was measured by the Temposonic device, and the trunnion forces were captured by the load cells. The plots and a discussion of these results follow.

Determination of System Responses

The results for shot #1 are shown in Figures 25 through 27. The preload for this shot was 2500 psi corresponding to an initial force of approximately 21,500 lbs. Figure 25 plots the gun's recoil position against time. At time zero the gun's position is at 17 inches (the FOOB start position). When the latch is released, the gun slowly begins to move forward. Very little motion is indicated for the first 0.020-sec. From 0.020- to approximately 0.090-sec, the accelerating gun moves towards the in-battery position. The displacement plot is quite smooth during this portion of the cycle. At 0.090-sec, at which the gun is 4.5 inches from the in-battery position, a low-magnitude "ripple" is indicated in the trace, which becomes more severe at 0.110-sec. At that time the gun is 2 inches from the in-battery position. This indicates that the counterrecoil buffer designed to arrest the gun in the event of a misfire has been activated. Remember the brakes provide very little resistance to motion during the working portion (from 17 to 4.5 inches) of run-up. The gun reaches the zero position at approximately 0.120-sec.

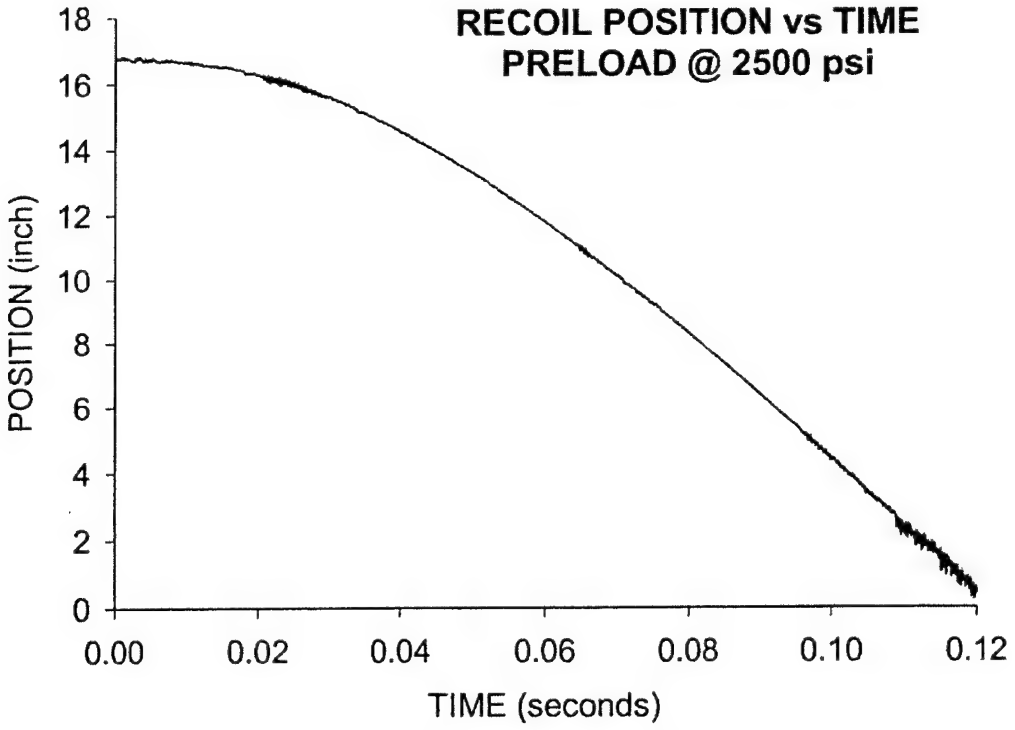

Figure 25. Recoil position versus time for run-up test shot #1.

Figure 26 shows the velocity for the test shot. Velocity was derived by differentiating the position data; therefore, some "noise" results from this process. Velocity begins at zero and decreases in a monotonic fashion to a terminal velocity of 200 in/sec at 0.100-sec. From this point forward, a large oscillation is indicated. Again, this is "noise" from the differentiation process. The salient information derived from this plot is the gun's terminal velocity. From the baseline test (reported previously), the gun's maximum recoil velocity was about 400 in/sec, twice the terminal velocity indicated in this test. This is exactly the level of run-up velocity needed to optimize the FOOB firings, and it is achieved at a recuperator preload of 2500 psi.

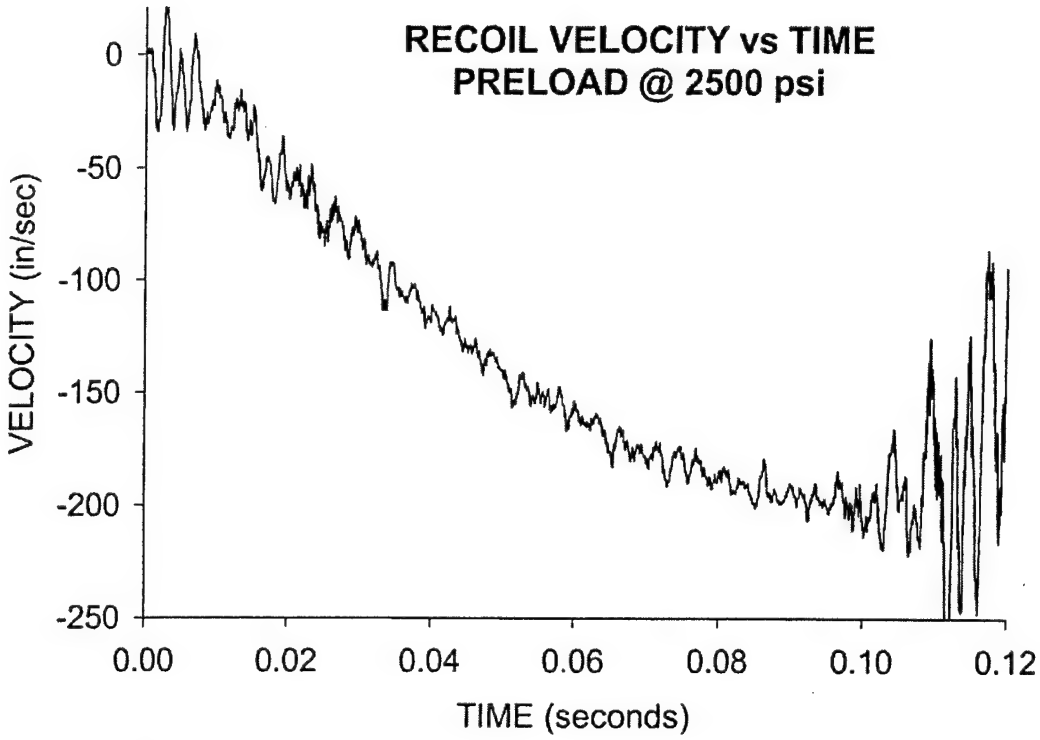

Figure 26. Recoil velocity versus time for run-up test shot #1.

Figure 27 depicts the total trunnion force data for this shot. The initial oscillation in this response is due to the abrupt nature in which the force is transferred to the mount upon release of the latch. The load cell, being an elastic member, responds appropriately to this suddenly-applied force. The actual level of the initial force is about 21,000 lbs, which is the recuperator preload value. This value is realized by averaging the first few cycles of the force oscillations. In general, the force decreases in time and mimics the decrease in recuperator force. At 0.090-sec the force levels off, then abruptly crosses the axis at 0.100-sec. This event indicates the activation of the counterrecoil safety buffer, which attempts to slow the forward motion eliminating the occurrence of a hard impact with the mount.

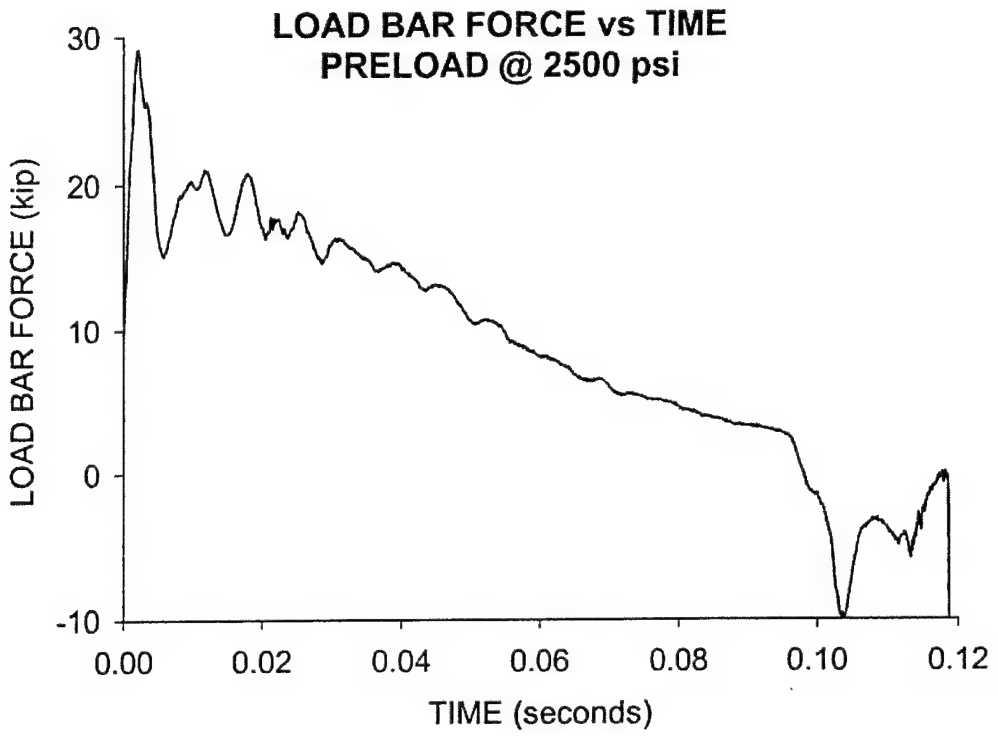

Figure 27. Trunnion force versus time for run-up test shot #1.

The results for shot #2 are shown in Figures 28 through 30. The preload for this shot was 1000 psi corresponding to a initial force of approximately 8700 lbs. Figure 28 plots the gun's recoil position against time. The response is similar to that of the previous test shot with the exception of the time duration. At this lower preload, the time needed to achieve a total travel of 17 inches is 0.200-sec. A minor discontinuity at 0.140-sec is probably due to electrical interference and not indicative of the overall response. The low and high "ripples" are indicated at the same location in travel, as shown in the previous test.

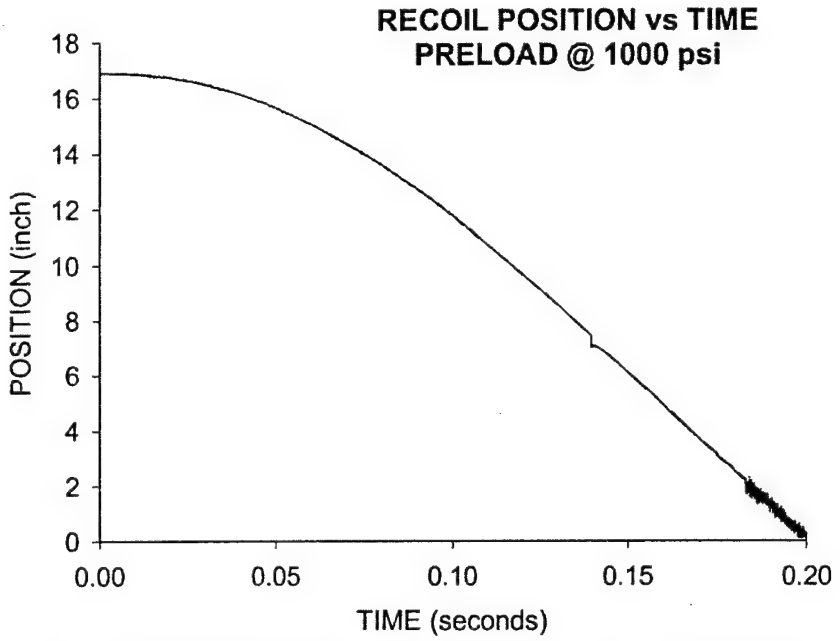

Figure 28. Recoil position versus time for run-up test shot #2.

Figure 29 shows the velocity for test shot #2. Terminal velocity for this shot is about 125 in/sec and occurs at 0.150-sec. The large spike at 0.140-sec is due to the erroneous data from the travel response.

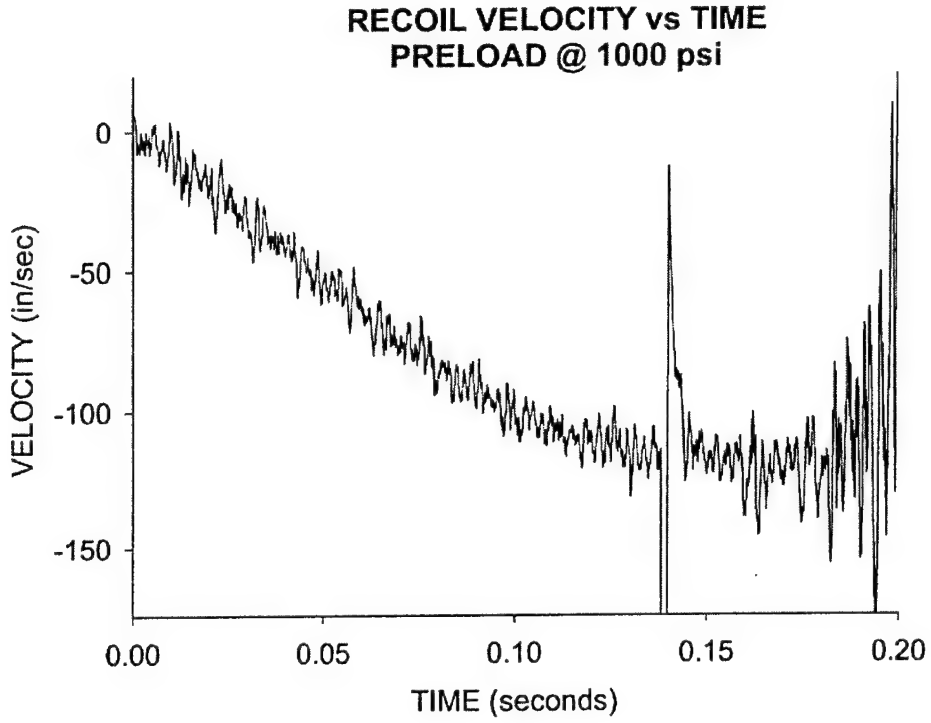

Figure 29. Recoil velocity versus time for run-up test shot #2.

Figure 30 illustrates the total trunnion force for test shot #2. Since the preload was only 1000 psi, the initial force indicated by the load cells was about 8100 lbs. Again, an initial oscillation is indicated along with a monotonic decrease up to 0.160-sec. The activation of the safety buffer is indicated by the quick reversal of the load direction at 0.175-sec. This test was very instrumental in establishing the level of preload needed, as well as the location for the ballistic pulse-triggering switch. Model validation of these test shots will be addressed next.

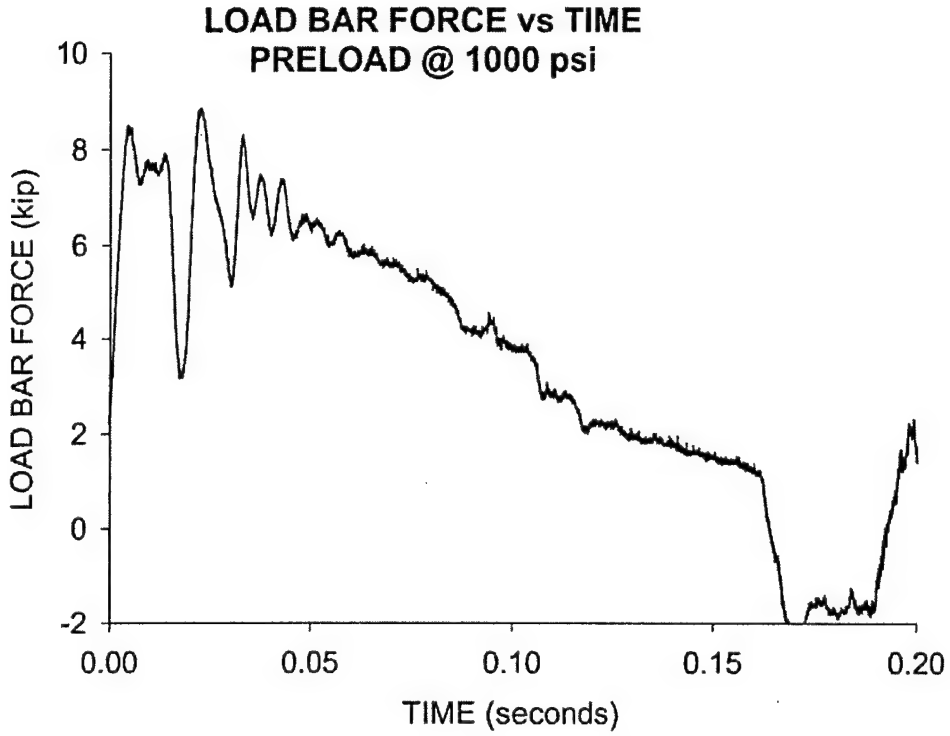

Figure 30. Trunnion force versus time for run-up test shot #2.

Comparison to Simulated Results

The simulated and test data results for shot #1 are shown in Figures 31 through 33. The preload for this shot was 2500 psi corresponding to a total force of approximately 21,500 lbs. Figure 31 shows a comparison of the displacement response. The smooth solid line curve represents the simulated results. The simulation model was run without additional friction (e.g., sliding surfaces between rails and cradle). Therefore, as the results indicate, the gun returns to its near-zero position about 0.005-sec quicker than the test shot. Other than that, the simulation and test results track very well. The slope changes abruptly at 0.117-sec, indicating a strong activation of the safety buffer. This is not shown in the test data, since its occurrence is outside the time window of the plot.

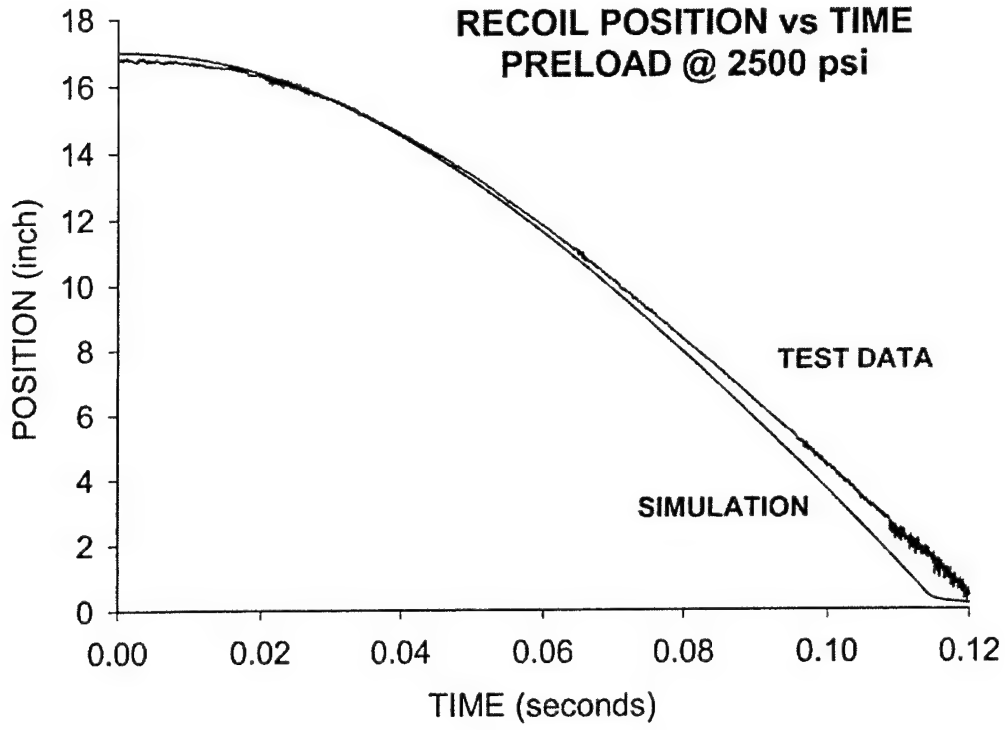

Figure 31. Recoil position versus time for run-up test shot #1 with simulated result.

Figure 32 shows a comparison of the velocity. The test data, as before, contain many "ripples" due to the differentiation process. The simulated result does not suffer from this, since velocity is derived from the integration of accelerating rather than the differentiation of travel. The peak run-up velocity as calculated from the model is about 225 in/sec, which is slightly greater than that of the test shot. However, the timing of both responses is very similar. Velocity terminates for both at about 0.115-sec.

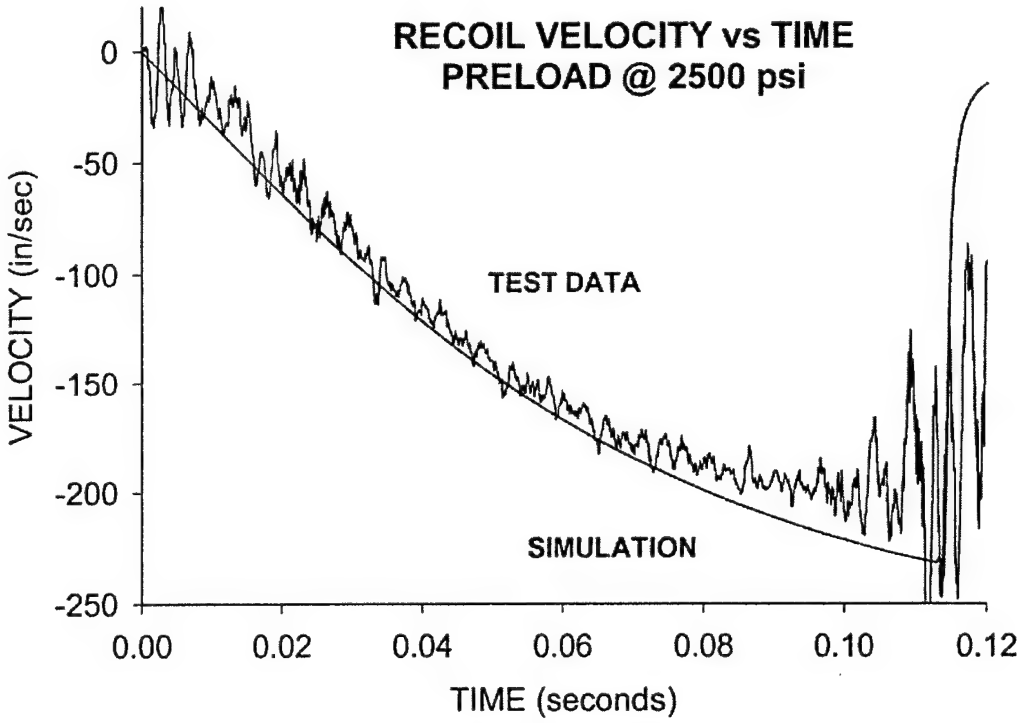

Figure 32. Recoil velocity versus time for run-up test shot #1 with simulated result.

Figure 33 illustrates a comparison of the trunnion force response. For this shot, the simulated result is slightly greater than that for the test shot by a few thousand pounds for most of the cycle. The reversal in force for the simulation occurs about 0.007-sec later and lacks the time distribution of the test shot. This is due to the model's treatment of the safety buffer. Since the exact amount and distribution of fluid initially in the buffer chamber is not known, both must be "guessed" prior to executing the simulation. If the guess is wrong, the force transfer near-zero will be erroneously calculated. (This would not occur for a standard fire in-battery simulation, since the amount of fluid that flows rearward to the buffer chamber is calculated based upon pressure and flow rate within the brake cylinder.)

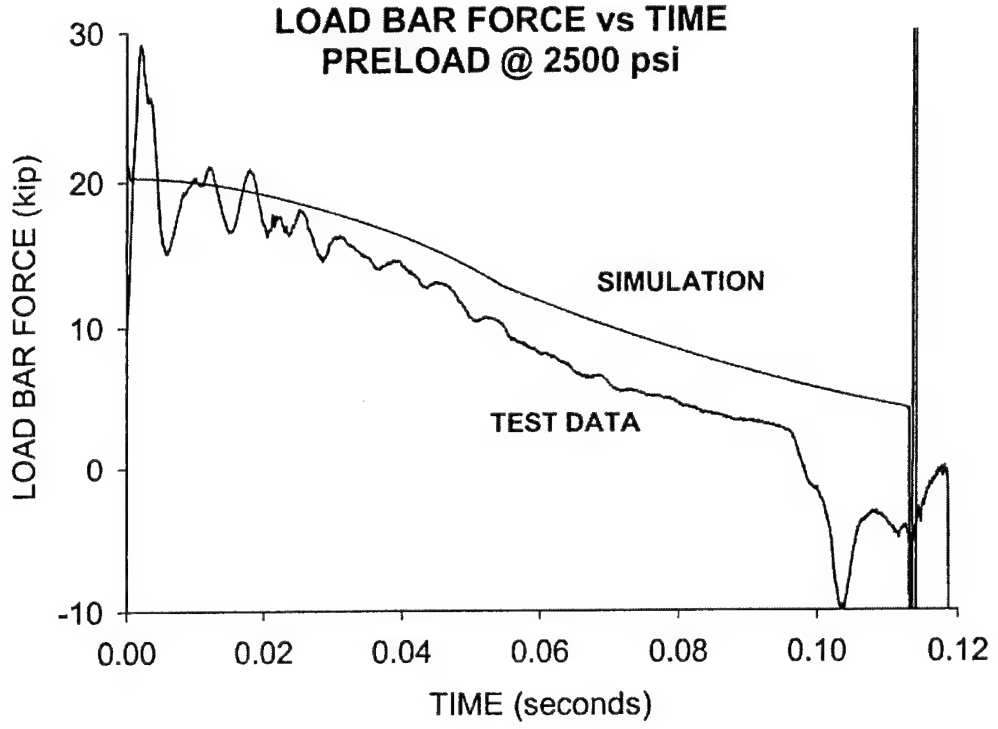

Figure 33. Trunnion force versus time for run-up test shot #1 with simulated result.

The simulated results and test data results for shot #2 are shown in Figures 34 through 36. The preload for this shot was 1000 psi corresponding to a total force of approximately 8700 lbs. Figure 34 shows recoil position versus time. Similar to the previous shot, the simulated result is slightly offset from the test shot; however, the discrepancy is not as great as that for the previous shot.

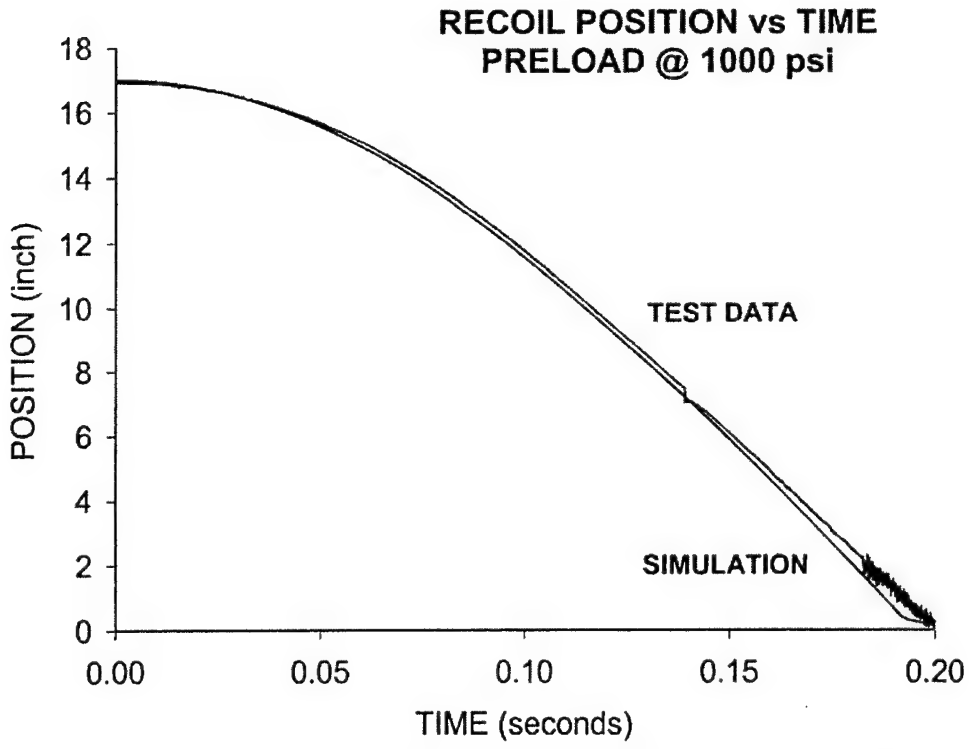

Figure 34. Recoil position versus time for run-up test shot #2 with simulated result.

Figure 35 shows the velocity responses. The simulated result tracks the data quite well for this shot. Both achieve a terminal velocity of approximately 140 in/sec at 0.190-sec.

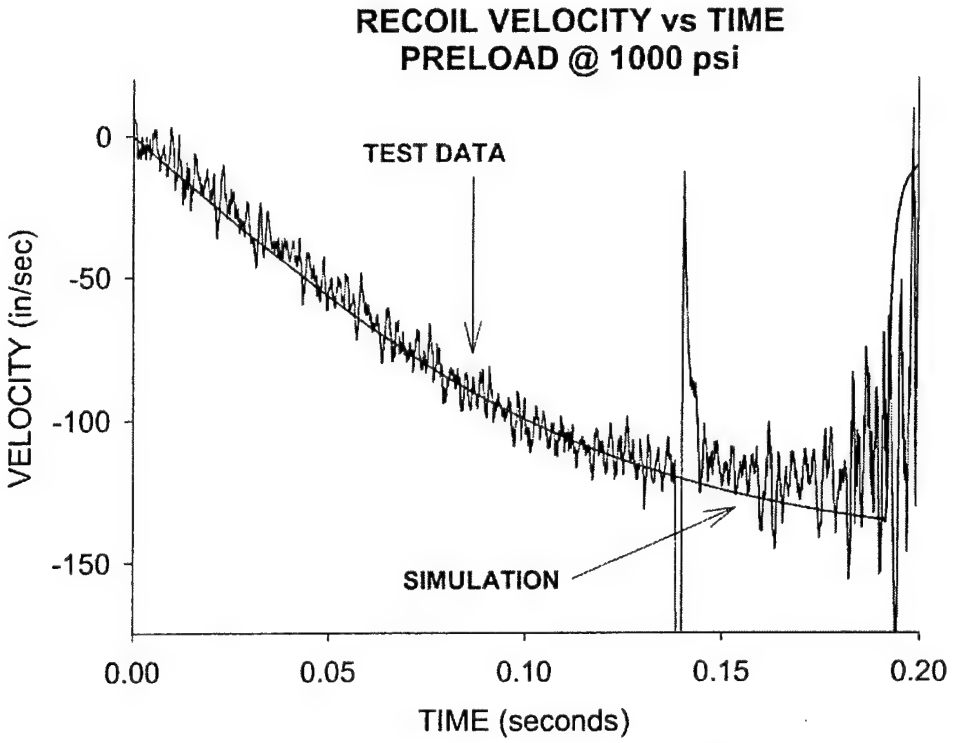

Figure 35. Recoil velocity versus time for run-up test shot #2 with simulated result.

The simulated result for the trunnion force response shown in Figure 36 is a better match for this shot. Both track each other up to the onset buffer activation. Test data indicate that the force abruptly changes direction at 0.170-sec, whereas the simulated results do not show force reversal until 0.190-sec.

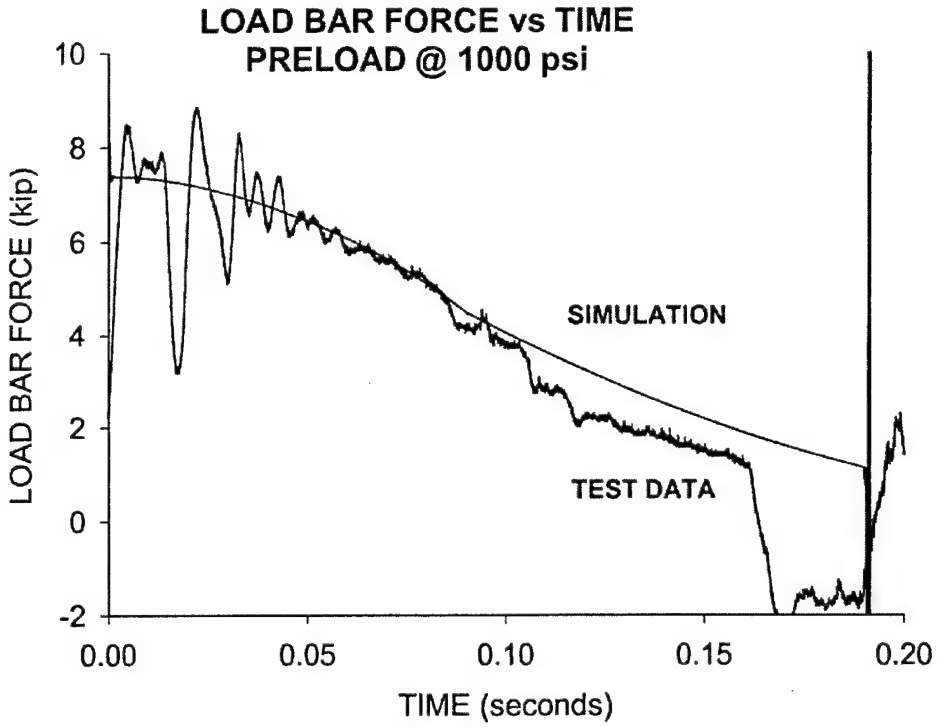

Figure 36. Trunnion force versus time for run-up test shot #2 with simulated result.

In general, the model tracked the data quite well for this test. Additionally, this indicates that the model could be used for fine-tuning the location of the ballistic trigger needed to energize the charge for FOOB firings. In the subsequent section, the results of the FOOB firings will be presented, discussed, and compared to simulations of the same.

FOOB TEST FOR M724 ROUND

Rationale for Test

The primary purpose for using a FOOB system is to reduce the recoil forces transferred to the vehicle through the trunnions. From the results of baseline firings, run-up tests, and recoil simulations, it was determined that a recuperator preload of approximately 2500 psi would reduce the trunnion forces from 35,000 lbs for standard firings of the M724 round to a value of 21,000 lbs when fired in FOOB mode. This is a 40 percent reduction. The primary concern in conducting successful FOOB firings is achieving a required run-up velocity and timing the application of the ballistic pulse to the forward-moving gun. We do not want a reduction in the run-up speed due to activation of the safety buffer, which (for this design) engages at four and one-half inches from the zero position, so the pulse must be initiated somewhat forward of this position. Using the results of the baseline firings, run-up test, and additional simulations, a

location for the firing trigger was determined for a 2500 psi preload. The average delay time from the initiation of the firing circuit until any dynamic activity due to ballistic pressure was 0.0098 sec (see Figure 14). Using this value and compensating for the forward momentum of the gun, the triggering mechanism was set to activate the firing circuit when the recoiling parts were seven and one-half inches from the zero position. Several live firings were conducted in which the preload was set between 2100 and 2500 psi. The results of these firings are presented and discussed below.

Determination of System Responses

Four preload values were used in the FOOB test firings. The displacement versus time plots are shown for representative shots of these four in Figure 37. These data are presented to show the effect that preload has upon the return location of the gun upon firing. It is hoped that the gun would return to its latch location; however, this was not the case for all shots. The upper left plot shows displacement for shot #1, which had a preload of 2500 psi. At time zero, the gun's position is 17 inches, which is the latch location. The gun is released and driven by the recuperator, moves forward. At the seven and one-half inch location, a slight blip is shown. This is electrical feedback from the firing pulse trigger and is indicated at the same location on all four plots. The firing circuit is activated at this time, and subsequently initiates burning of the primer and then the main charge. Note that the gun continues forward for another three plus inches at which time the ballistic pressure is great enough to overcome the forward momentum of the gun and reverse its direction. This occurs at a time of 0.100-sec. The gun returns along a trajectory very similar to its run-up; however, its peak displacement is about 15 inches, which is a few inches short of the latch location, thus the gun does not relatch. When the preload was reduced to 2300 psi for test shot #5, the displacement trajectory as shown in the plot at the upper right did return to the latch position of 17 inches. This plot is quite symmetric about the time value of 0.112-sec. When the preload was reduced further, as indicated in the lower plots (shots #13 and #17), the return stroke increased inversely with preload. At 2100 psi the gun traveled to 17.8 inches, which is 0.8-inch past the latch position. For shots #5 and #13, the return stroke was just enough for the gun to relatch. For shot #1 the gun did not recoil far enough and for shot #17 it recoiled too far. For shot #17, which recoiled 0.8-inch past the latch position, the latch mechanism could not manage the excessive forward velocity of the gun due to its override position. Upon impact the latch released and the gun moved forward being arrested by the safety buffer in the recoil brakes and the external snubbers on the rear face of the cradle. (This portion of the stroke is not shown in the figures.) Additional design work is needed to render the latch more robust and to control the velocity of the gun when it recoils past the latch location.

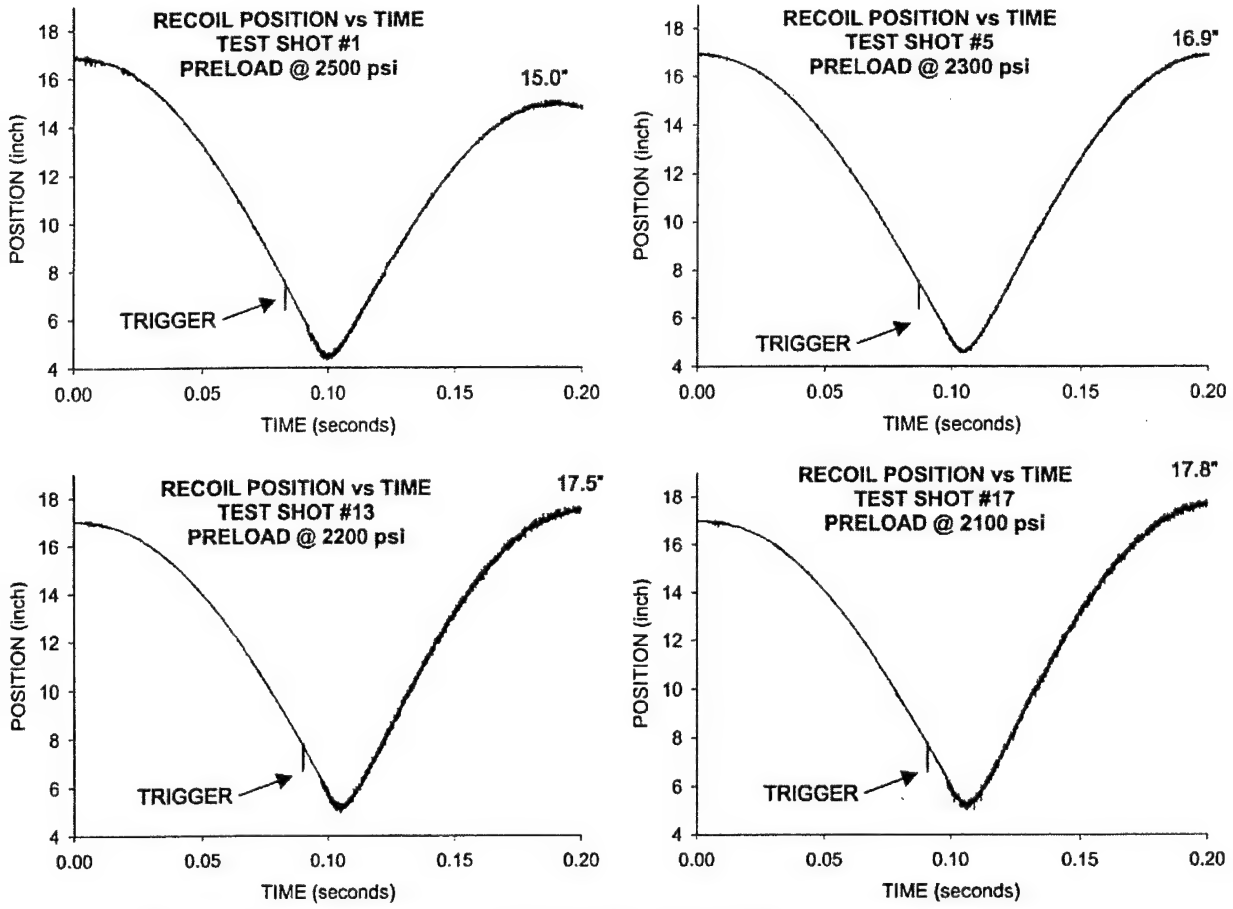

Figure 37. Recoil position versus time for FOOB test, four separate shots.

Figure 38 shows the velocity versus time plots for the same four FOOB shots. Since velocity was derived by a numeric differentiation of the displacement data, a great deal of numerically-induced noise is indicated. The plot in the top left corner corresponds to shot #1 at a preload of 2500 psi. Velocity begins at zero (as expected) and monotonically decreases to about 200 in/sec at 0.090-sec. The large "blip" at 0.085-sec is indicative of firing circuit activation in the displacement data. Just short of 0.100-sec, the velocity quickly reverses and within 0.020-sec increases to about 200 in/sec in the recoil direction. From this point forward, gun speed returns to zero in much the same fashion as in the earlier portion of the cycle. In subsequent shots for which the preload was reduced, the velocity trajectories are similar, but velocity levels in the run-up portion are slightly less. This makes sense since speed should be directly proportional to preload. For shots #5, #13, and #17, the peak run-up velocities are 180, 170, and 160 in/sec, respectively. For the return stroke, the peak velocities increase with decreasing preload.

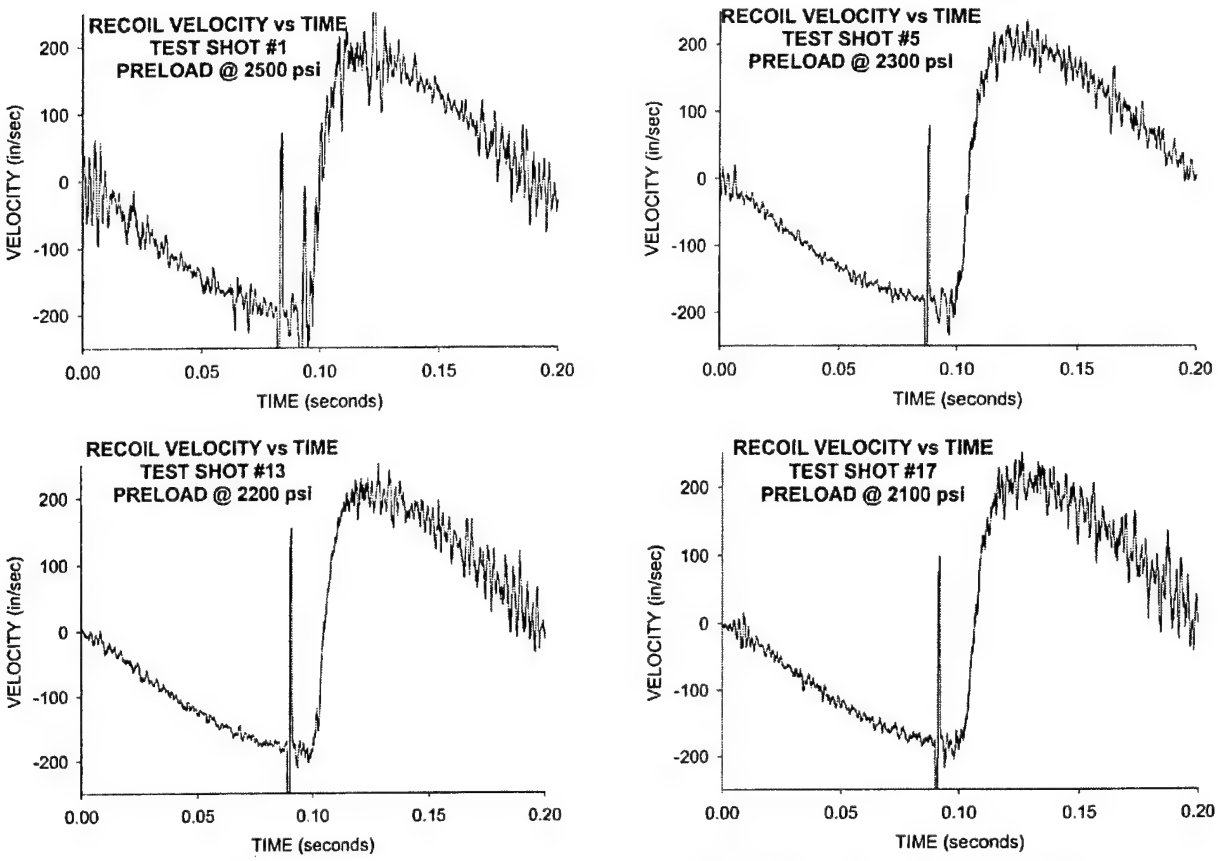

Figure 38. Recoil velocity versus time for FOOB test, four separate shots.

Figure 39 illustrates the total trunnion force versus time plots for these same four FOOB shots. The bulk of the trunnion force is due to the recuperator load, since the brakes have been designed to provide very little resistance during the active portion of the FOOB recoil stroke. For shot #1, as indicated in the top left plot, the force begins at about 21,800 lbs. Note the oscillation in the initial portion of the plot. This is due to the sudden nature of the applied load during unlatch. The force transducers being elastic tend to oscillate for a few cycles. The force gradually reduces as the gun moves forward reaching a minimum of 3000 lbs at 0.095-sec. Upon application of the ballistic load, the gun stops abruptly and reverses direction. The load cells initially respond (again elastically) in an oscillatory manner until a monotonic increase to 18,800 lbs is indicated at 0.175-sec. A similar response is shown for the remaining FOOB shots with initial force levels corresponding to their preload. For shots #5, #13, and #17, the initial force is 20,100, 19,200, and 18,300 lbs, respectively. The comparable maximum forces for the return stroke are 19,000, 19,200, and 19,600 lbs, respectively. The goal of FOOB firings is to return the recoiling parts to their initial position. In this position, the trunnion force (being location-dependent only) is exactly equal to the preload of the recuperators. A comparison of these test results to the simulated responses will be discussed next.

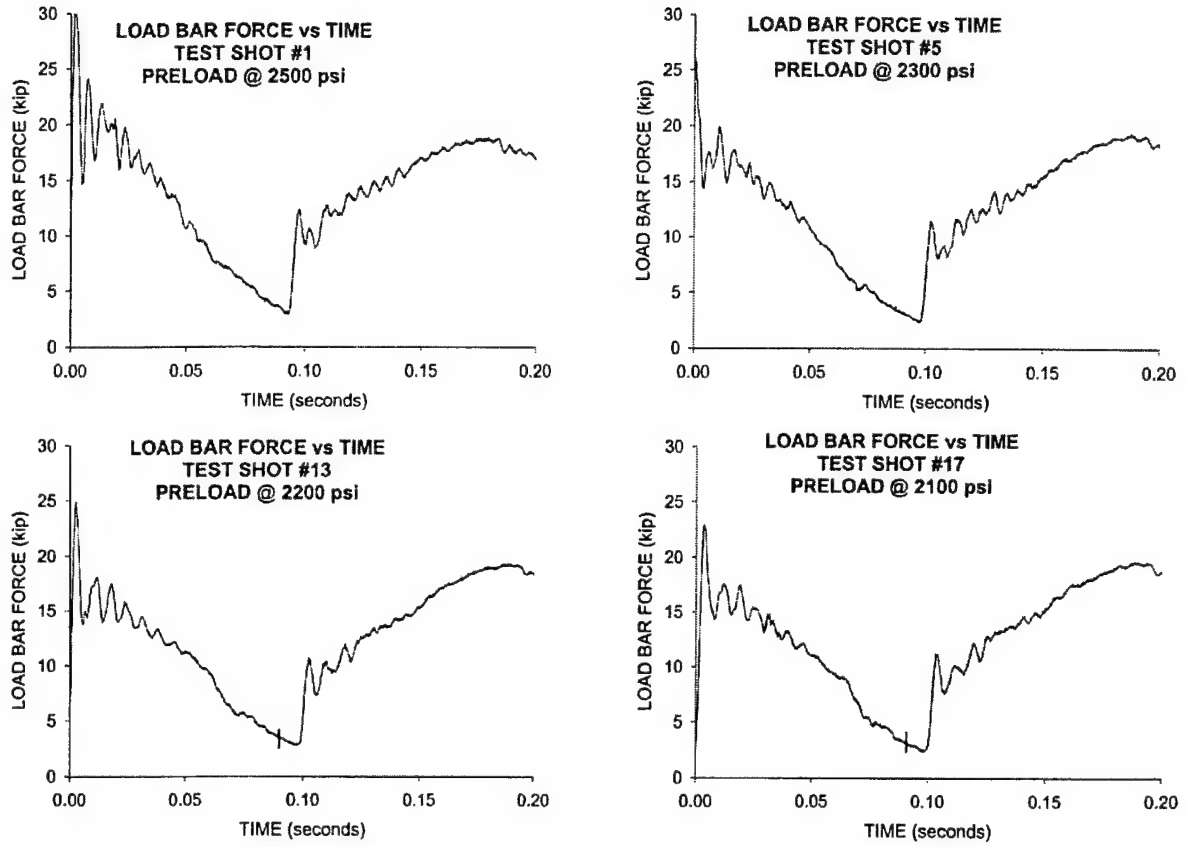

Figure 39. Trunnion force versus time for FOOB test, four separate shots.

Comparison to Simulated Results

Figure 40 again shows the displacement versus time plots for the four FOOB shots with the simulated responses superimposed. As indicated in all four cases, the simulated responses for the run-up portion of the displacement trajectory match the test data quite well. For shot #1 (upper left plot), the location of the minimum displacement (approximately 4.5 inches) is the same for both the test data and simulation; however, the timing for the simulation is early by about 0.004-sec. Upon return in recoil, the simulated response is offset from the data by about one inch on the high side for the full-length of the stroke. The simulation predicts that the return to the stationary location is 16 inches, one inch greater than the test data. A potential explanation for this discrepancy is the fact that the friction between sliding (rails) and stationary (mount channels) surfaces was not included in the simulations. The force level for this type of friction was not determined for this gun system. The remaining three shots indicate discrepancies in both location of the displacement reversal (i.e., minimum location) and the stationary return point in recoil. The discrepancy in minimum location is likely due to the uncertainty in timing of pressure buildup in the chamber. Note that during baseline testing, the range of timing values between firing circuit activation and ballistic activity was 0.005-sec. This causes an uncertainty

of about one inch in the location of initial pressure buildup in the chamber at speeds of 200 in/sec. For all three shots the difference between minimum location of the test data and simulations is about one inch. The timing for the simulations is always quicker than for the test, since a fixed value of timing offset was used for all simulations. Compounding this with the fact that sliding friction is unknown and not included in the simulations renders a spatial and temporal offset in the recoil portion of the displacement plots, in some cases by as much as two inches and 0.005-sec at the stationary recoil location. (Each test shot could have been examined for timing and included as part of the simulations if further refinement were warranted.) The results of these comparisons beg for either a tighter tolerance on shot initiation (propellant issue) or a more robust latch design (mechanical issue) that may tolerate overshoots without loss of function.

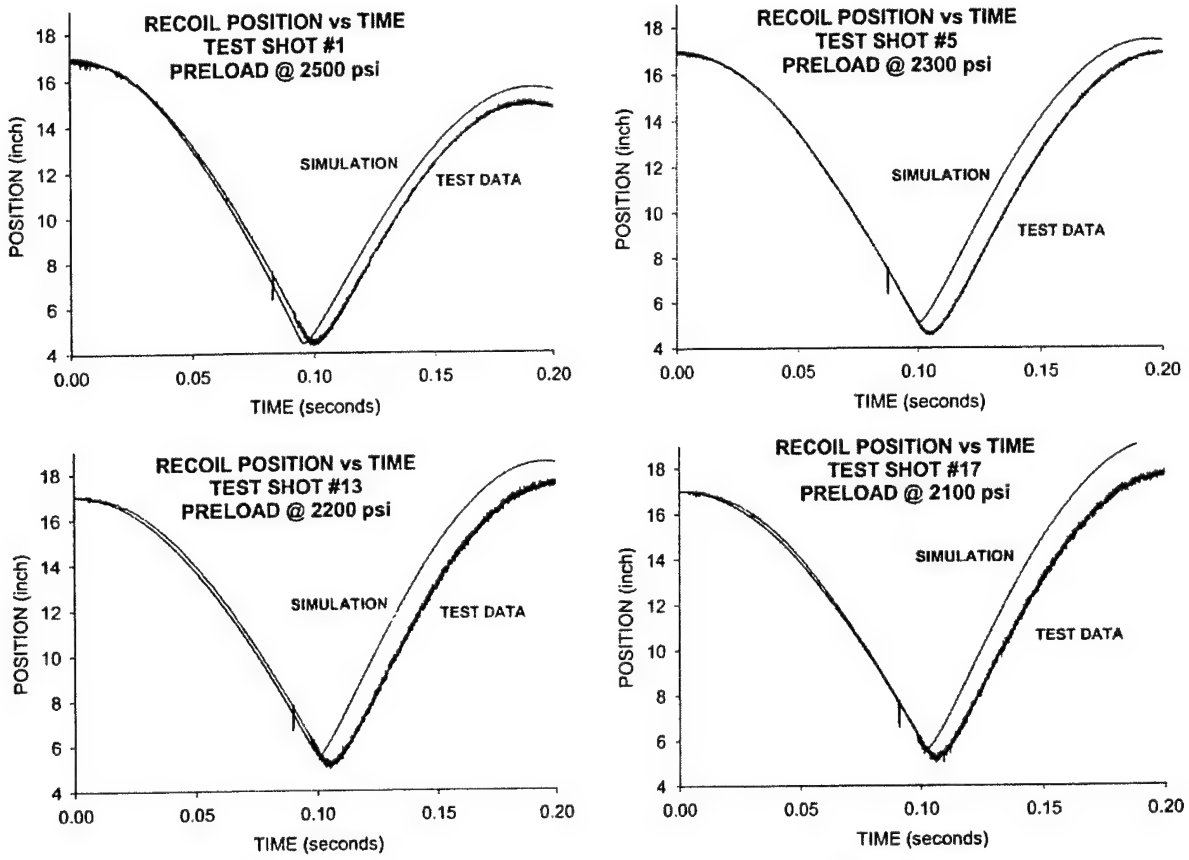

Figure 40. Recoil position versus time comparison with FOOB test, four separate shots.

Figure 41 again depicts the recoil velocity versus time plots for the four FOOB shots with the simulated responses superimposed. The solid smooth line represents the simulated response, whereas the solid oscillating line represents the test data. The most striking characteristic of these comparisons is that during the run-up portion of the shot, the simulated response matches the test data quite well. If one were to calculate a running average for the test data (using several data points in the process) during run-up, it would be very close to the simulated response. (Heavier filtering and/or averaging of the displacement data before differentiation would have accomplished the same result, thus rendering a better match of the simulated response.) After shot initiation and the short time during which the gun reverses direction, the simulated velocity response rises much quicker than that of the test data. This again indicates a misunderstanding of the shot initiation process. (Note: the ballistic pressure/time data used in the simulations were derived from computer modeling using a standard universally accepted code. It assumes that all propellant grains begin burning simultaneously that, in reality, is not the case.) This timing discrepancy is another contributor to the divergence between the test and simulated displacement response during recoil. During the remaining portion of recoil (after the ballistic pulse has decayed), the simulated response and test data match quite well.

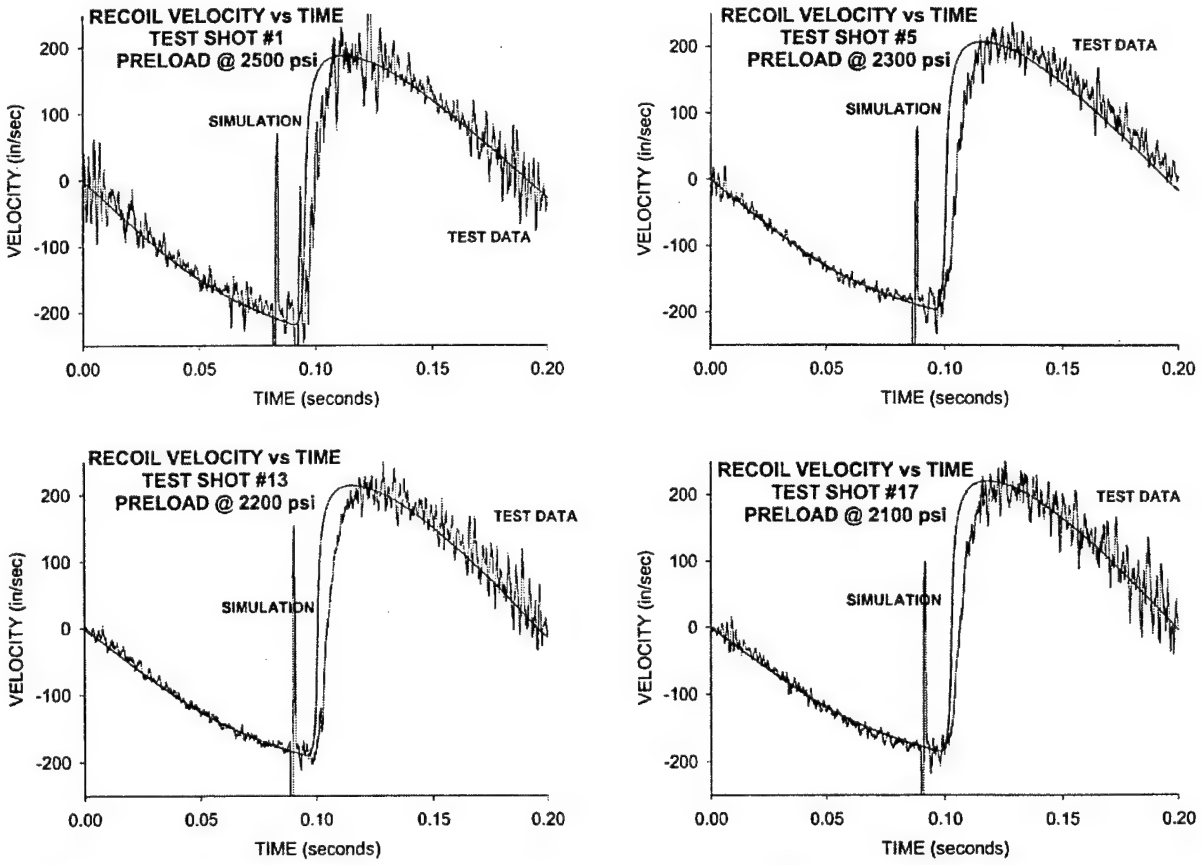

Figure 41. Recoil velocity versus time comparison with FOOB test, four separate shots.

Figure 42 presents the trunnion force versus time plots for the four FOOB shots, along with the simulated responses superimposed. The shapes of all four test responses are similar to the simulations; however, in all cases, the simulated response overshoots the test data, in one case by as much as 4000 lbs. Most likely cause of the discrepancy is a lack of knowledge of sliding friction. Friction forces are applied in a direction opposite those of the recuperator forces, thus would subtract from the load felt at the trunnions. The only shot for which a match occurs is for the recoil portion of the shot depicted in the upper left plot. All the rest suffer from the offset discrepancy.

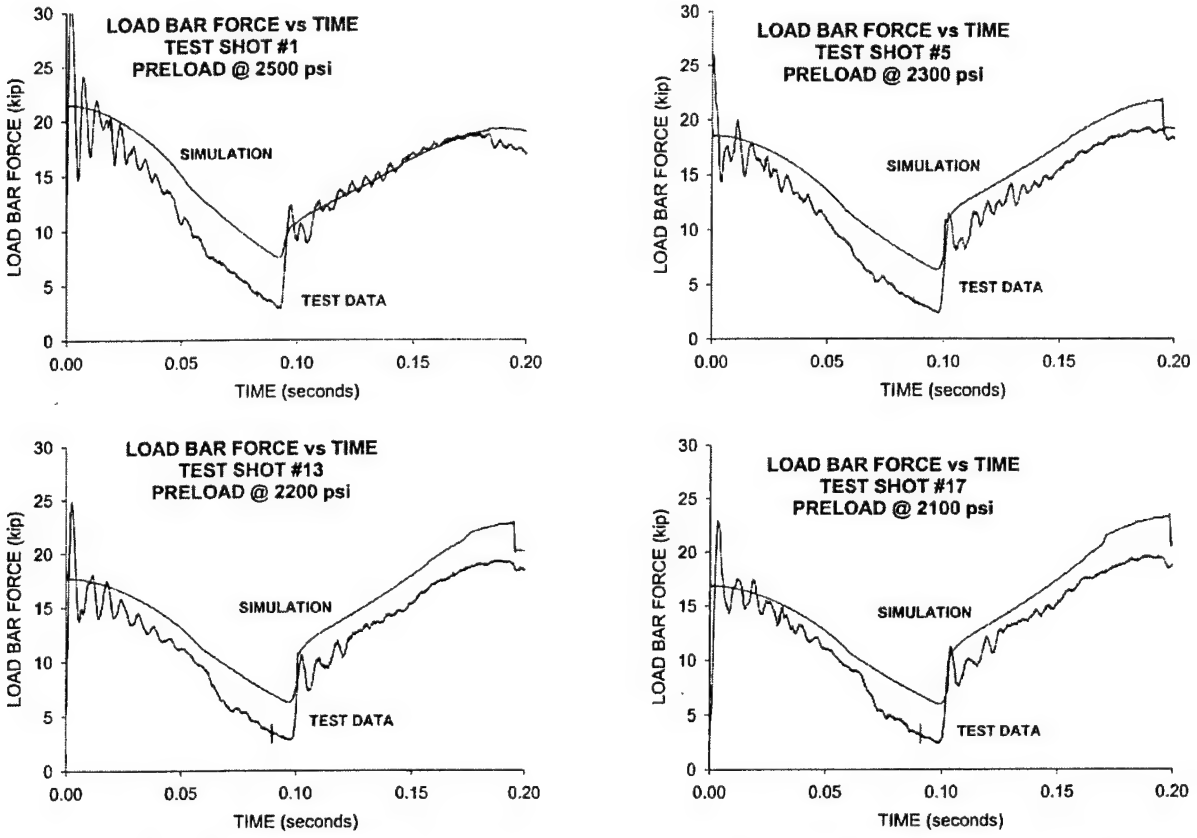

Figure 42. Trunnion force versus time comparison with FOOB test, four separate shots.

In general, given the uncertainty in sliding friction and accurate modeling of the propellant burning process, especially during the initial burn phase, the simulated responses represent the test data quite well. Further refinement of the model would include using actual ballistic pressure data and timing for each shot. Additionally, offline testing could be conducted on the weapon to determine the friction forces that develop between the gun rails and mount guides. Both of these system-dependent results could easily be applied to the model using standard input functions.

CONCLUSIONS

Reiterating, the purpose of firing a cannon in a FOOB mode is to reduce the forces transmitted to the mount or vehicle. By using a slightly modified version of the 105-mm M35 tank gun, we were able to illustrate this for a direct-fire weapon. Explaining in detail the operation of both systems provided a reasonable comparison between the kinematical operation of conventional and FOOB systems. Our design metrics, however, were driven by cost constraints in that the number of new parts or modifications of old parts must be minimized. The only modification we felt was needed for the FOOB system was the design of a new control rod profile and buffer plug for the brakes. The recuperator was used as-is at an increased preload. Accommodations for overshoot of the latch were not considered. This, of course, did not address the robustness of the latch design, which as indicated, was defeated several times during the FOOB firings. (The latch assembly was purchased off-the-shelf from Rock Island Arsenal.) Our main goals were to demonstrate an electronic shot ignition system that was robust in terms of its repeatability and that firing in a FOOB mode reshaped and reduced the forces transmitted to its support structure. Both of these goals were met.

Considerable design, simulation, and test work was conducted prior to any FOOB firings. The Benet Labs Recoil Simulation Programs, which have been used in the design and analysis of several recoil systems for both direct and indirect fire applications, had to be modified and tested to allow for FOOB operation. Restating, in a FOOB setting, the firing simulation starts with the gun captured in its out-of-battery position with respect to conventional operation. When the gun is unlatched and under considerable preload from the recuperator, it accelerates forward toward an electrical trigger, which initiates the ballistic cycle. The location of this trigger was determined using simulation, while accommodating the average delay time of a typical M724 round. This delay time was acquired from baseline testing. Additional information acquired from the baseline test was the value of the impulse delivered by the M724 round. This was accomplished by integration in time of the load-bar data, as well as a redundant calculation using the pressure data from the brakes and recuperators. The difference between the two was about 7 percent, assumed to be the loss of a friction component not recordable by the brakes or recuperators.

The dynamic nature of the load bars was indicated in the test as well. The load bars being elastic respond as such when initially subjected to a load applied at a high rate. The brakes, which provide a bulk of the retarding force, respond in a short time period (~5 ms), thus to the load bars this appears as a step function, and a few oscillations around a mean value are indicated. The difficulty in calculating recoil velocity by numerically differentiating the displacement data was shown. Considerable filtering of the displacement data was required to produce a reasonable velocity response. However, as a result of subsequent simulations of the recoiling weapon, considerable confidence was instilled in the use of computer modeling to determine the responses of this system. The calculated dynamic and kinematic values for both recoil and counterrecoil tracked the data quite well.

Prior to executing FOOB firings, a nonfiring test was conducted at WMC to gather data that would verify the model's capability in predicting the kinematics of the gun during the run-up portion of the cycle. The FOOB brakes were installed, and the two run-up preload pressure values were used in the test. At a preload of 2100 lbs, the maximum forward velocity achieved was 125 in/sec, whereas at a preload of 2500 lbs, the velocity was 200 in/sec. For these same cases, the model's prediction was slightly greater, probably due to the absence of friction in the model. Based upon these results, the FOOB simulations were fine-tuned to establish the exact location of the firing trigger switch and the preload needed to optimize the FOOB test. A 2500 psi preload and a trigger location of seven and one-half inches from the in-battery position were selected for initial FOOB firings.

For the FOOB test, the latch was located as indicated above; however, four preload values were tested. These values were 2100, 2200, 2300, and 2500 psi, respectively. Test results indicated that the 2200 and 2300 psi preloads were just enough to return the gun to its latch location and not cause an override of its function. At 2500 psi, the gun did not recoil past the latch location, and at 2100 psi, the gun recoiled about one inch past the latch position, thus upon return, the latch released and the gun's motion was arrested by the forward buffers and external snubbers. The simulated responses (displacement, velocity, and load-bar force) for the same were very good indicators of the test in a global sense; however, due to the lack of knowledge of shot initiation, there were localized discrepancies between the two. The comparison of displacement during run-up was quite good, yet at shot initiation, both time and location offsets appeared. These offsets were also evident in the velocity and load-bar responses as well.

In conclusion, FOOB would be a viable option for a direct-fire weapon if shot initiation were more robust and less uncertain. Additionally, control of the gun whenever it recoils past the latch position is needed such that its return speed does not defeat the function of the latch mechanism.

REFERENCES

1. Kathe, E., and Gast, R., "A Fire Out-Of-Battery Tank Gun: Theory and Simulation," ARDEC Technical Report ARCCB-TR-02007, Benet Laboratories, Watervliet, NY, May 2002.

2. Gast, R.G., "Exploitation of the T-62 Recoil System's Operational Characteristics," ARDEC Technical Report ARCCB-TR-88007, Benet Laboratories, Watervliet, NY, February 1988.

3. Gast, R.G., "Determination of Muzzle Brake Efficiency for the EX35 Gun System," Benet Laboratories Internal Technical Report BITR No. 89-7, Benet Laboratories, Watervliet, NY, November 1989.

TECHNICAL REPORT INTERNAL DISTRIBUTION LIST

	NO. OF COPIES
TECHNICAL LIBRARY ATTN: AMSTA-AR-CCB-O	1
TECHNICAL PUBLICATIONS & EDITING SECTION ATTN: AMSTA-AR-CCB-O	3
PRODUCTION PLANNING & CONTROL DIVISION ATTN: AMSTA-WV-ODP-Q, BLDG. 35	1

NOTE: PLEASE NOTIFY DIRECTOR, BENÉT LABORATORIES, ATTN: AMSTA-AR-CCB-O OF ADDRESS CHANGES.

TECHNICAL REPORT EXTERNAL DISTRIBUTION LIST

	NO. OF COPIES
DEFENSE TECHNICAL INFO CENTER ATTN: DTIC-OCA (ACQUISITIONS) 8725 JOHN J. KINGMAN ROAD STE 0944 FT. BELVOIR, VA 22060-6218	2
COMMANDER U.S. ARMY TACOM-ARDEC ATTN: AMSTA-AR-WEE, BLDG. 3022 AMSTA-AR-AET-O, BLDG. 183 AMSTA-AR-FSA, BLDG. 61 AMSTA-AR-FSX AMSTA-AR-FSA-M, BLDG. 61 SO AMSTA-AR-WEL-TL, BLDG. 59 PICATINNY ARSENAL, NJ 07806-5000	 1 1 1 1 1 2
DIRECTOR U.S. ARMY RESEARCH LABORATORY ATTN: AMSRL-DD-T, BLDG. 305 ABERDEEN PROVING GROUND, MD 21005-5066	 1
DIRECTOR U.S. ARMY RESEARCH LABORATORY ATTN: AMSRL-WM-MB (DR. B. BURNS) ABERDEEN PROVING GROUND, MD 21005-5066	 1
CHIEF COMPOSITES & LIGHTWEIGHT STRUCTURES WEAPONS & MATLS RESEARCH DIRECT U.S. ARMY RESEARCH LABORATORY ATTN: AMSRL-WM-MB (DR. BRUCE FINK) ABERDEEN PROVING GROUND, MD 21005-5066	 1
COMMANDER U.S. ARMY RESEARCH OFFICE ATTN: TECHNICAL LIBRARIAN P.O. BOX 12211 4300 S. MIAMI BOULEVARD RESEARCH TRIANGLE PARK, NC 27709-2211	 1
COMMANDER ROCK ISLAND ARSENAL ATTN: SIORI-SEM-L ROCK ISLAND, IL 61299-5001	 1
COMMANDER U.S. ARMY TANK-AUTMV R&D COMMAND ATTN: AMSTA-DDL (TECH LIBRARY) WARREN, MI 48397-5000	 1
COMMANDER U.S. MILITARY ACADEMY ATTN: DEPT OF CIVIL & MECH ENGR WEST POINT, NY 10966-1792	 1
U.S. ARMY AVIATION AND MISSILE COM REDSTONE SCIENTIFIC INFO CENTER ATTN: AMSAM-RD-OB-R (DOCUMENTS) REDSTONE ARSENAL, AL 35898-5000	 2
NATIONAL GROUND INTELLIGENCE CTR ATTN: DRXST-SD 2055 BOULDERS ROAD CHARLOTTESVILLE, VA 22911-8318	 1

NOTE: PLEASE NOTIFY COMMANDER, ARMAMENT RESEARCH, DEVELOPMENT, AND ENGINEERING CENTER, BENÉT LABORATORIES, CCAC, U.S. ARMY TANK-AUTOMOTIVE AND ARMAMENTS COMMAND, AMSTA-AR-CCB-O, WATERVLIET, NY 12189-4050 OF ADDRESS CHANGES.